Proceedings of the Institution of Mechanical Engineers, Part G: Journal of Aerospace Engineering, ***2018, Vol 232, Issue 5, pp884–901***
First published date: April-03-2017
doi: 10.1177/0954410017699236

Application of Lyapunov matrix inequality based unsymmetrical saturated control to a multi-vectored propeller airship

Li Chen[1], James F. Whidborne[2], Qi Dong[3] and Deng Ping Duan [4]

[1,4]*School of Aeronautics and Astronautics, Shanghai Jiao Tong University, P.R China*

[2]*Centre for Aeronautics, School of Aerospace, Transport and Manufacturing, Cranfield University, UK*

[3]*MuDanJiang Medical University, P.R China*

Abstract: The problem of the design of a controller for a multi-vectored propeller airship is addressed. The controller includes anti-windup that takes into account unsymmetrical actuator constraints. First, a linear transformation is applied to transform the unsymmetrical constraints into symmetric constraints with an amplitude-bounded exogenous disturbance. Then, a stability condition based on a quadratic Lyapunov function for the saturated closed-loop system is proposed. The condition considers both amplitude-bounded and energy-bounded exogenous disturbances. Thus the controller design problem is transformed into a convex optimization problem expressed in a bilinear matrix inequality form. Two

Corresponding author:
Li Chen, School of Aeronautics and Astronautics,
Shanghai Jiaotong University, No. 800, Dongchuan Road, Shanghai
200240, China.
Email: chen2006@sjtu.edu.cn

controller design methods were applied: one-step controller and traditional Anti-Windup Controller (AWC). The one-step method obtains the controller and the anti-windup compensator in one step while the AWC method separates this process into the linear controller design and the compensator design. Simulation results showed that both controllers enlarge the stability zone of the saturation system and have good tracking performance. It is shown that the AWC design method not only has a larger region of stability, but the demanded actuator output exceeds the constraints less and has a smaller anti-windup coefficient matrix compared to the one-step method.

Keywords: multi-vectored propeller airship, unsymmetrical saturation, one-step controller anti-windup controller, LMI

Notation

$\mathbf{a} \in R^{m\times m}$ Actuator upper limits matrix

a_i The i^{th} element of $\mathbf{a}$ matrix

$\mathbf{b} \in R^{m\times m}$ Actuator lower limits matrix

b_i The i^{th} element of $\mathbf{b}$ matrix

$\boldsymbol{u} \in R^m$ Actuator input vector

$\boldsymbol{u}_0 \in R^m$ Actuator symmetric limits vector

$\boldsymbol{w}_{\text{p}} \in R^q$ Bounded energy exogenous signal

$\boldsymbol{w}_{\xi} \in R^q$ Bounded amplitude disturbance

$\boldsymbol{x}_{\text{p}} \in R^n$ System state vector

$\boldsymbol{x}_c \in R^{n_c}$ Controller state vector

$\boldsymbol{y}_{\mathrm{p}} \in R^{p}$ Measured output vector

$\boldsymbol{y}_{\mathrm{c}} \in R^{m}$ Controller asymmetric output

$\bar{\boldsymbol{y}}_{\mathrm{c}} \in R^{m}$ Controller symmetric output

$\boldsymbol{z} \in \boldsymbol{R}^{r}$ Regulated output vector

$\mathbf{G} \in R^{m \times n}$ Designed matrix

$\mathbf{I}_{\mathbf{n}}$ Identity matrix of dimensions $\boldsymbol{n} \times \boldsymbol{n}$

$\mathbf{0}_{\mathbf{n}}$ Null matrix of dimensions $\boldsymbol{n} \times \boldsymbol{n}$

$\mathbf{K} \in R^{m \times n}$ State feedback matrix

$\mathbf{P} \in R^{n \times n}$ Symmetric positive definite matrix

$\beta^{-1} > 0$ Admissible initial states size

$\gamma^{-1} > 0$ System L_2-gain

$\delta^{-1} > 0$ Admissible energy bounded disturbance size

$\delta_{\xi}^{-1} > 0$ Admissible amplitude bounded disturbance size

$\eta^{-1} > 0$ Admissible states size

$\boldsymbol{\xi}$ Column vector whose components are all equal to 1

$\tau_1 > 0, \tau_2 > 0$ The designed positive parameters

1. Introduction

The stability and the stabilization of systems including saturations is an important field of research in control theory [1, 2]. The presence of a saturation may be a source of instability, or at least of only local stability, and frequently implies a reduction of the performances [3, 4].

In the literature, the stabilization problems for linear systems with saturating controls can classified into two main approaches: saturation avoidance and saturation allowance. The first one consists of control laws in order to avoid control saturation [5-8], while the second one handles the occurrence of the control saturation and stabilizes larger region of stability, thus receiving more attention in the literature [9-12]. In this context, these works can be divided into two approaches: the one-step controller and the traditional Anti-Windup Controller (AWC) [13]. The one-step controller is designed simultaneously taking into account performance specification and a safe domain of operation. Higher performance may be expected if a controller is designed a priori considering the saturation effect, however, the solutions offered by optimal control techniques tend to be complex and unintuitive [14-17]; The anti-windup controller allows separation in design of the controller devoted to achieving nominal performance and the compensator devoted to constraint handling [4,18-20]. The AWC technique is considered attractive in practice because no restriction is placed upon the nominal linear controller when no saturation is encountered.

When the open-loop system is exponentially unstable or when some performance or robustness specifications should be met, for the closed-loop saturated system, only local stabilization is possible [21,22]. In this case, the characterization of sets of admissible initial states and admissible disturbances plays a central role in stability analysis and synthesis. Thanks to more sophisticated modeling of the saturation nonlinearities including polytopic models and sector nonlinearity models, major improvements in this field have been achieved associated with using quadratic and polyhedral Lyapunov functions to build regions of stability [11-20], more detailed results related to this area have been stated in seminal works of Tarbouriech and her co-authors [11-15, 20,22]. They presented proofs of

these theories in terms of stabilization of saturated system and their solutions of estimated basin of attraction, and designed controller were given based on the use of linear programming and convex optimization problems with LMI constraints [23].

In this paper, an application of Tarbouriech's theory to a multi-vectored propeller airship is presented. The control problem addressed is one of an over-actuated system with unsymmetrical actuator saturation constraints. Firstly, for the constraints can be expressed in an LMI form, a linear transformation is applied to transfer the unsymmetrical constraints into symmetric constraints with an amplitude-bounded exogenous disturbance [24]. The stabilization theory from [13, pp.149-150] is then extended to take into account simultaneous amplitude-bounded and energy-bounded exogenous disturbance. Subsequently the controller design problem is transformed into a convex optimization problem expressed in several LMI forms. A one-step controller and a traditional anti-windup controller are then computed in a similar manner as [13, pp.293-297, 14]. Simulation results demonstrate the possibility of application of the two methods to this airship.

2. Saturation nonlinearity models

2.1 Linear systems subject to unsymmetrical constraints

In this section, we show the system can be modelled as an unsymmetrical saturation with exogenous signal, $\boldsymbol{w}_{\mathrm{p}}$. This signal can be considered as a disturbance, a tracking reference or a combination of both. Hence, we consider that the open-loop system is generically represented as:

$$\begin{aligned} \dot{\boldsymbol{x}}_{\mathrm{p}} &= \mathbf{A}_{\mathbf{p}}\boldsymbol{x}_{\mathrm{p}} + \mathbf{B}_{\mathbf{pu}}\boldsymbol{u} + \mathbf{B}_{\mathbf{pw}}\boldsymbol{w}_{\mathrm{p}} \\ \boldsymbol{y}_{\mathrm{p}} &= \mathbf{C}_{\mathbf{p}}\boldsymbol{x}_{\mathrm{p}} + \mathbf{D}_{\mathbf{pu}}\boldsymbol{u} + \mathbf{D}_{\mathbf{pw}}\boldsymbol{w}_{\mathrm{p}} \\ \boldsymbol{z} &= \mathbf{C}_{\mathbf{pz}}\boldsymbol{x}_{\mathrm{p}} \end{aligned} \tag{1}$$

where $\boldsymbol{x}_{\mathrm{p}} \in R^{n}$ is the state vector, $\boldsymbol{u} \in R^{m}$ is the control vector , $\boldsymbol{y}_{\mathrm{p}} \in R^{p}$ is the measured output vector, $\boldsymbol{z} \in \boldsymbol{R}^{r}$ is the regulated output vector, $\boldsymbol{w}_{\mathrm{p}} \in R^{q}$ is input exogenous signal, $\mathbf{A_p}, \mathbf{B_{pu}}, \mathbf{B_{pw}}, \mathbf{C_p}, \mathbf{D_{pu}}$ and $\mathbf{D_{pw}}$ are real matrices of appropriate dimensions.

Consider that the exogenous signal $\boldsymbol{w}_{\mathrm{p}}(t)$ is energy bounded, i.e. it belongs to the following set of functions:

$$W_{\mathrm{p}} = \{\boldsymbol{w}_{\mathrm{p}} : [0,\infty] \to R^{q}; \int_{0}^{\infty} \boldsymbol{w}_{\mathrm{p}}(\tau)' \mathbf{R} \boldsymbol{w}_{\mathrm{p}}(\tau) d\tau \le \delta^{-1}\} \tag{2}$$

for some $\delta > 0$, with $\mathbf{R} = \mathbf{R}^{\mathbf{T}} > 0$. In this case the energy of $\boldsymbol{w}_{\mathrm{p}}(t)$ is bounded by δ^{-1}. We assume that a dynamic output stabilizing compensator

$$\begin{aligned} \dot{\boldsymbol{x}}_{\mathrm{c}} &= \mathbf{A_c}\boldsymbol{x}_{\mathrm{c}} + \mathbf{B_c}\boldsymbol{y}_{\mathrm{p}} \\ \boldsymbol{y}_{\mathrm{c}} &= \mathbf{C_c}\boldsymbol{x}_{\mathrm{c}} + \mathbf{D_c}\boldsymbol{y}_{\mathrm{p}} \end{aligned} \tag{3}$$

is applied to system (1). Due to the magnitude bounds, the effective control signal provided by the actuator can be modelled by a saturation function, that is

$$\dot{\boldsymbol{x}}_{\mathrm{p}} = \mathbf{A_p}\boldsymbol{x}_{\mathrm{p}} + \mathbf{B_{pu}}\mathrm{sat}(\boldsymbol{y}_{\mathrm{c}}) + \mathbf{B_{pw}}\boldsymbol{w}_{\mathrm{p}} \tag{4}$$

where each component of the control vector, $\boldsymbol{u}$, can be described by

$$u_i = \mathrm{sat}(y_{ci}) = \begin{cases} a_i & if \quad y_{ci} > a_i \\ y_{ci} & if \; b_i \le y_{ci} \le a_i \\ b_i & if \quad y_{ci} < b_i \end{cases} \tag{5}$$

for $i = 1, \cdots, m$ where y_{ci} is the i^{th} output of the controller, and a_i, b_i are the upper limit and lower limits of the i^{th} actuator respectively, noting that for many real systems their absolute values are not equal. For the constraints to be expressed under LMI form, following [24], a new variable is introduced to convert the unsymmetrical control $\boldsymbol{y}_c$ into a symmetrical control $\bar{\boldsymbol{y}}_{\mathrm{c}}$ and a constant disturbance term so that

$$\bar{\boldsymbol{y}}_{\mathrm{c}} = \boldsymbol{y}_{\mathrm{c}} - \frac{\mathbf{a}+\mathbf{b}}{\mathbf{2}}\boldsymbol{\xi} \tag{6}$$

where **a** and **b** are matrix with diagonal elements a_i and b_i respectively and $\boldsymbol{\xi}$ is column vector whose components are all equal to 1.

The asymmetrical saturation is linked to the symmetric saturation by

$$\text{sat}(\bar{\boldsymbol{y}}_c) = \text{sat}(\boldsymbol{y}_c) - \frac{\mathbf{a}+\mathbf{b}}{\mathbf{2}}\boldsymbol{\xi} \tag{7}$$

where $\text{sat}(\bar{\boldsymbol{y}}_c)$ is considered as the symmetrical saturation control, where each component of the control vector is defined by

$$\text{sat}(\bar{y}_{ci}) = \begin{cases} u_{0i} & if \quad \bar{y}_{ci} > u_{0i} \\ \bar{y}_{ci} & if -u_{0i} \le \bar{y}_{ci} \le u_{0i} \\ -u_{0i} & if \quad \bar{y}_{ci} < -u_{0i} \end{cases} \tag{8}$$

where u_{0i} is the i^{th} component of vector $\boldsymbol{u}_0$ and $\boldsymbol{u}_0 = \frac{\mathbf{a}-\mathbf{b}}{\mathbf{2}}\boldsymbol{\xi}$.

Equation (6) can be rewritten as follows

$$\boldsymbol{y}_c = \bar{\boldsymbol{y}}_c - \mathbf{D}_{c\xi}\boldsymbol{w}_\xi \tag{9}$$

with matrix $\mathbf{D}_{c\xi} = -\sqrt{m}\left(\frac{\mathbf{a}+\mathbf{b}}{\mathbf{2}}\right)$ and $\boldsymbol{w}_\xi = \frac{\boldsymbol{\xi}}{\sqrt{m}}$, where *m* is the number of the control variables. We can now rewrite the state equation of system (1) as

$$\begin{aligned} \dot{\boldsymbol{x}}_p &= \mathbf{A}_p\boldsymbol{x}_p + \mathbf{B}_{pu}\text{sat}(\bar{\boldsymbol{y}}_c) + \mathbf{B}_{p\xi}\boldsymbol{w}_\xi + \mathbf{B}_{pw}\boldsymbol{w}_p \\ \boldsymbol{y}_p &= \mathbf{C}_p\boldsymbol{x}_p + \mathbf{D}_{pu}\text{sat}(\bar{\boldsymbol{y}}_c) + \mathbf{D}_{p\xi}\boldsymbol{w}_\xi + \mathbf{D}_{pw}\boldsymbol{w}_p \\ \boldsymbol{z} &= \mathbf{C}_{pz}\boldsymbol{x}_p \end{aligned} \tag{10}$$

with matrices $\mathbf{B}_{p\xi} = -\mathbf{B}_{pu}\mathbf{D}_{c\xi}$, $\mathbf{D}_{p\xi} = -\mathbf{D}_{pu}\mathbf{D}_{c\xi}$, and $\boldsymbol{w}_\xi^T\boldsymbol{w}_\xi = \delta_\xi^{-1} = 1$. The obtained system (10) can be seen as a symmetric saturated system with a bounded amplitude disturbance $\boldsymbol{w}_\xi$ and bounded energy disturbance $\boldsymbol{w}_p$.

2.2 Classical and generalized sector condition

Let us define the actuator dead-zone nonlinearity by $\boldsymbol{\phi}(\bar{\boldsymbol{y}}_c) = \text{sat}(\bar{\boldsymbol{y}}_c) - \bar{\boldsymbol{y}}_c$, from this definition, the closed-loop system (10) can be written as [13]

$$\begin{aligned}\dot{\boldsymbol{x}}_{\mathrm{p}} &= \mathbf{A}_{\mathbf{p}}\boldsymbol{x}_{\mathrm{p}} + \mathbf{B}_{\mathbf{pu}}\bar{\boldsymbol{y}}_{\mathrm{c}} + \mathbf{B}_{\mathbf{p}\xi}\boldsymbol{w}_{\xi} + \mathbf{B}_{\mathbf{pw}}\boldsymbol{w}_{\mathbf{p}} + \mathbf{B}_{\mathbf{pu}}\boldsymbol{\phi}(\bar{\boldsymbol{y}}_{\mathbf{c}}) \\ \boldsymbol{y}_{\mathrm{p}} &= \mathbf{C}_{\mathbf{p}}\boldsymbol{x}_{\mathbf{p}} + \mathbf{D}_{\mathbf{pu}}\bar{\boldsymbol{y}}_{\mathbf{c}} + \mathbf{D}_{\mathbf{p}\xi}\boldsymbol{w}_{\xi} + \mathbf{D}_{\mathbf{pw}}\boldsymbol{w}_{\mathbf{p}} + \mathbf{D}_{\mathbf{pu}}\boldsymbol{\phi}(\bar{\boldsymbol{y}}_{\mathbf{c}}) \\ \boldsymbol{z} &= \mathbf{C}_{\mathbf{pz}}\boldsymbol{x}_{\mathbf{p}}\end{aligned} \tag{11}$$

For all $\bar{\mathbf{y}}_{\mathbf{c}} \in R^m$, the nonlinearity $\boldsymbol{\phi}(\bar{\mathbf{y}}_{\mathbf{c}})$ satisfies the following inequality [13]:

$$\boldsymbol{\phi}(\bar{\boldsymbol{y}}_{\boldsymbol{c}})^{\mathrm{T}}\mathbf{T}(\boldsymbol{\phi}(\bar{\boldsymbol{y}}_{\boldsymbol{c}}) + \bar{\boldsymbol{y}}_{\boldsymbol{c}}) \le 0 \tag{12}$$

for any diagonal positive definite matrix $\mathbf{T} \in R^{m\times m}$.This inequality is a classical sector condition which is globally verified, i.e., it is verified for $\bar{\mathbf{y}}_{\mathbf{c}} \in R^m$. Now we state a generalized sector condition, its use should result in less conservative conditions than the use of classical sector conditions. Define the following set [13]

$$S(\bar{\boldsymbol{y}}_{\mathrm{c}} - \boldsymbol{y}_{\mathrm{g}}, \boldsymbol{u}_0) = \left\{\bar{\boldsymbol{y}}_{\mathrm{c}} \in R^m, \boldsymbol{y}_{\mathrm{g}} \in R^m \mid -\boldsymbol{u}_0 \le \bar{\boldsymbol{y}}_{\mathrm{c}} - \boldsymbol{y}_{\mathrm{g}} \le \boldsymbol{u}_0\right\} \tag{13}$$

If $\bar{\boldsymbol{y}}_{\mathrm{c}}$ and $\boldsymbol{y}_{\mathrm{g}}$ are elements of $S(\bar{\boldsymbol{y}}_{\mathrm{c}} - \boldsymbol{y}_{\mathrm{g}}, \boldsymbol{u}_0)$, then the nonlinearity $\boldsymbol{\phi}(\bar{\boldsymbol{y}}_{\mathrm{c}})$ satisfies the following inequality [13]:

$$\boldsymbol{\phi}(\bar{\boldsymbol{y}}_{\mathrm{c}})^{T}\mathbf{T}(\boldsymbol{\phi}(\bar{\boldsymbol{y}}_{\mathrm{c}}) + \boldsymbol{y}_{\mathrm{g}}) \le 0 \tag{14}$$

Note that the sector condition (14) is more general than (12). In fact $\boldsymbol{y}_{\mathrm{g}}$ appears as an extra degree of freedom in the stability conditions. The generalized sector condition allows one to convexify the anti-windup synthesis problem for regional (local) stability [13]. Applying state feedback $\bar{\boldsymbol{y}}_{\mathrm{c}} = \mathbf{K}\boldsymbol{x}_{\boldsymbol{p}}$, and choosing $\boldsymbol{y}_{\mathrm{g}} = \bar{\boldsymbol{y}}_{\mathrm{c}} + \mathbf{G}\boldsymbol{x}_{\boldsymbol{p}}$, $\mathbf{G} \in R^{m\times n}$, the set defined by equation (13) becomes

$$S(\left|\bar{\boldsymbol{y}}_{\mathrm{c}} - \boldsymbol{y}_{\mathrm{g}}\right|, \boldsymbol{u}_0) = \{\boldsymbol{x}_{\boldsymbol{p}} \in R^n; \left|\mathbf{G}\boldsymbol{x}_{\boldsymbol{p}}\right| \le \boldsymbol{u}_0\} \tag{1}$$

5)

The state deduced from condition (15) is the allowed state of the saturated system with a certain saturation allowance. The sector nonlinearity $\boldsymbol{\phi}(\bar{\boldsymbol{y}}_{\mathrm{c}})$ satisfying inequality (14) becomes [13]:

$$\boldsymbol{\phi}(\bar{\boldsymbol{y}}_{\mathrm{c}})^{\mathrm{T}}\mathbf{T}(\boldsymbol{\phi}(\bar{\boldsymbol{y}}_{\mathrm{c}}) + \bar{\boldsymbol{y}}_{\mathrm{c}} + \mathbf{G}\boldsymbol{x}) < 0 \tag{16}$$

Consider the quadratic Lyapunov function $V(\boldsymbol{x}) = \boldsymbol{x}^{\mathrm{T}}\mathbf{P}\boldsymbol{x}$ with $\mathbf{P} = \mathbf{P}^{\mathrm{T}} > \mathbf{0}$, the regions of asymptotic stability is given by the ellipsoidal domains defined as follows:

$$\varepsilon(\mathbf{P},\eta) = \{\boldsymbol{x} \in R^n; \boldsymbol{x}^{\mathrm{T}}\mathbf{P}\boldsymbol{x} \le \eta^{-1}\} \quad \text{with} \quad \eta > 0 \tag{17}$$

If the ellipsoid $\varepsilon(\mathbf{P},\eta)$ is included in the polyhedral set $S(\left|\bar{y}_{\mathrm{c}} - y_{\mathrm{g}}\right|, \boldsymbol{u}_0)$, then the following linear matrix inequality is satisfied [13]:

$$\begin{bmatrix} \mathbf{P} & \boldsymbol{G}_i^{\mathrm{T}} \\ \boldsymbol{G}_i & \eta \mathrm{u}_{0i}^2 \end{bmatrix} \ge 0, i = 1 \cdots m \tag{18}$$

where $\boldsymbol{G}_i$ is the i^{th} row of matrix $\mathbf{G}$.

3. Stability analysis and stabilization

3.1 Anti-windup compensator synthesis

In order to mitigate the undesirable effects of windup caused by input saturation, an anti-windup term $\boldsymbol{v} = \left[\boldsymbol{v}_{\mathrm{x}}^{\mathrm{T}} \quad \boldsymbol{v}_{\mathrm{y}}^{\mathrm{T}}\right]^{\mathrm{T}}$ can be added to the controller (3). The control structure is as shown in Fig.1 [13]

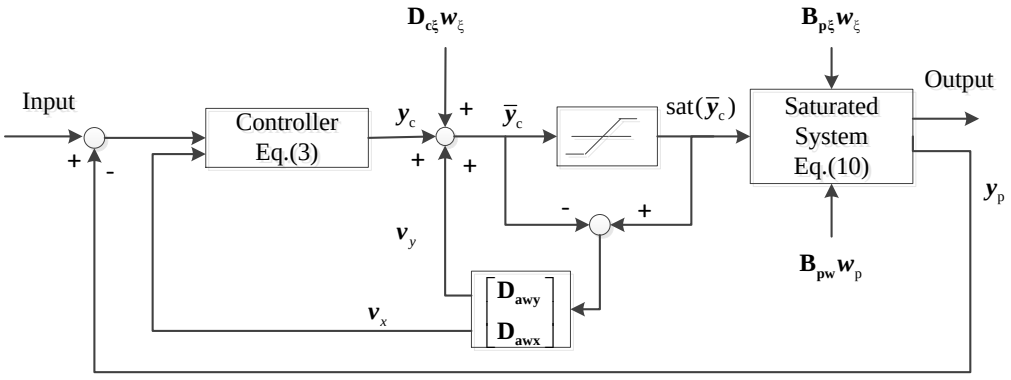

Fig.1 Anti-windup compensator synthesis

Although anti-windup compensation has been mainly related to performance improvement, it can also be used to enlarge the region of attraction (or an estimate of it) of the saturated closed-loop system. Hence, the anti-windup problem can be generically defined as follows.

$$\begin{aligned} \dot{\boldsymbol{x}}_{\mathrm{c}} &= \mathbf{A}_{\mathbf{c}}\boldsymbol{x}_{\mathrm{c}} + \mathbf{B}_{\mathbf{c}}\boldsymbol{y}_{\mathrm{p}} + \boldsymbol{v}_{\mathbf{x}} \\ \boldsymbol{y}_{\mathrm{c}} &= \mathbf{C}_{\mathbf{c}}\boldsymbol{x}_{\mathrm{c}} + \mathbf{D}_{\mathbf{c}}\boldsymbol{y}_{\mathrm{p}} + \boldsymbol{v}_{\mathbf{y}} \end{aligned} \tag{19}$$

The non-symmetric saturation control is linked to the symmetric saturation control:

$$\begin{aligned} \dot{\boldsymbol{x}}_{\mathrm{c}} &= \mathbf{A}_{\mathbf{c}}\boldsymbol{x}_{\mathbf{c}} + \mathbf{B}_{\mathbf{c}}\boldsymbol{y}_{\mathbf{p}} + \mathbf{D}_{\mathbf{awx}}\boldsymbol{\phi}(\bar{\boldsymbol{y}}_{\mathrm{c}}) \\ \bar{\boldsymbol{y}}_{\mathrm{c}} &= \mathbf{C}_{\mathbf{c}}\boldsymbol{x}_{\mathrm{c}} + \mathbf{D}_{\mathbf{c}}\boldsymbol{y}_{\mathbf{p}} + \mathbf{D}_{\mathbf{c}\xi}\boldsymbol{w}_{\xi} + \mathbf{D}_{\mathbf{awy}}\boldsymbol{\phi}(\bar{\boldsymbol{y}}_{\mathrm{c}}) \end{aligned} \tag{20}$$

Thus considering the dynamic controller and this anti-windup strategy, the closed-loop system is

$$\begin{aligned} \dot{\boldsymbol{x}} &= \mathbf{A}\boldsymbol{x} + \mathbf{B}\boldsymbol{\phi}(\bar{\boldsymbol{y}}_{\mathrm{c}}) + \mathbf{B}_{\mathbf{w}}\boldsymbol{w}_{\mathrm{p}} + \mathbf{B}_{\xi}\boldsymbol{w}_{\xi} \\ \bar{\boldsymbol{y}}_{\mathrm{c}} &= \mathbf{C}\boldsymbol{x} + \mathbf{D}\boldsymbol{\phi}(\bar{\boldsymbol{y}}_{\mathrm{c}}) + \mathbf{D}_{\mathbf{w}}\boldsymbol{w}_{\mathrm{p}} + \mathbf{D}_{\xi}\boldsymbol{w}_{\xi} \\ \boldsymbol{z} &= \mathbf{C}_{\mathbf{z}}\boldsymbol{x} \end{aligned} \tag{21}$$

where

$$\boldsymbol{x} = \begin{bmatrix} \boldsymbol{x}_{\mathbf{p}}^{\mathrm{T}} & \boldsymbol{x}_{\mathbf{c}}^{\mathrm{T}} \end{bmatrix}^{\mathrm{T}} \in R^{n+m}, \quad \mathbf{A} = \begin{bmatrix} \mathbf{A}_{\mathbf{p}} + \mathbf{B}_{\mathbf{pu}}\mathbf{D}_{\mathbf{c}}\mathbf{C}_{\mathbf{p}} & \mathbf{B}_{\mathbf{pu}}\mathbf{C}_{\mathbf{c}} \\ \mathbf{B}_{\mathbf{c}}\mathbf{C}_{\mathbf{p}} & \mathbf{A}_{\mathbf{c}} \end{bmatrix}, \mathbf{B} = \begin{bmatrix} \mathbf{B}_{\mathbf{pu}} + \mathbf{B}_{\mathbf{pu}}[\mathbf{0} \quad \mathbf{I}_{\mathbf{m}}]\mathbf{D}_{\mathbf{aw}} \\ \begin{bmatrix} \mathbf{I}_{\mathbf{n_c}} & \mathbf{0} \end{bmatrix}\mathbf{D}_{\mathbf{aw}} \end{bmatrix},$$

$$\mathbf{B}_{\mathbf{w}} = \begin{bmatrix} \mathbf{B}_{\mathbf{pw}} \\ \mathbf{0} \end{bmatrix}, \mathbf{B}_{\xi} = \begin{bmatrix} \mathbf{B}_{\mathbf{pu}}\mathbf{D}_{\mathbf{c}\xi} + \mathbf{B}_{\mathbf{p}\xi} \\ \mathbf{B}_{\mathbf{c}}\mathbf{D}_{\mathbf{p}\xi} \end{bmatrix}, \mathbf{C} = \begin{bmatrix} \mathbf{D}_{\mathbf{c}}\mathbf{C}_{\mathbf{p}} & \mathbf{C}_{\mathbf{c}} \end{bmatrix}, \mathbf{D} = \mathbf{0}, \mathbf{D}_{\mathbf{w}} = \mathbf{0}, \mathbf{D}_{\xi} = \mathbf{D}_{\mathbf{c}\xi},$$

$$\mathbf{C}_{\mathbf{z}} = [\mathbf{C}_{\mathbf{pz}} \quad \mathbf{0}], \mathbf{B}_1 = \begin{bmatrix} \mathbf{B}_{\mathbf{pu}} \\ \mathbf{0} \end{bmatrix}, \mathbf{B}_2 = \begin{bmatrix} \mathbf{B}_{\mathbf{pu}}[\mathbf{0} \quad \mathbf{I}_{\mathbf{m}}] \\ \begin{bmatrix} \mathbf{I}_{\mathbf{n_c}} & \mathbf{0} \end{bmatrix} \end{bmatrix}.$$

3.2 Input-to-state stability analysis

Since the closed-loop system (21) is nonlinear, the action of the exogenous signal can produce trajectories that converge to equilibrium points other than the origin, to limit cycles, or can even diverge [13]. In this case we are interested in determining sets of "admissible" exogenous signals. These admissible sets are in general characterized with respect to bounds on the amplitude (L_∞-norm) and/or the energy (L_2-norm) of the disturbance. This problem is also referred to as input-to-state stability analysis [13].

Problem 1 Given a set of admissible initial states $\boldsymbol{x}_0$ and admissible disturbances set defined for a specified class of signals $\boldsymbol{w}_{\mathrm{p}}(t) \in W_{\mathrm{p}}$, determine a control law $\boldsymbol{u}$(t) such that:

1. The trajectories of the closed-loop system (21) are bounded, i.e., they are confined in some compact set *R*.

2. If the disturbance is vanishing, then $\lim_{t\to\infty} \boldsymbol{x}(t)=0$.

3. Given a set W_{p} of admissible exogenous signals and a regulated output $\boldsymbol{z}(t)$, minimize the upper bound for the L_2-gain from $\boldsymbol{w}_{\mathrm{p}}(t)$ to $\boldsymbol{z}(t)$:

$$L_2 = \sup_{\|\mathbf{w_p}\|_2^2 \neq 0} \frac{\|\boldsymbol{z}\|_2^2}{\|\boldsymbol{w}_{\mathbf{p}}\|_2^2}, \text{ considering here that } \eta=\delta \tag{22}$$

Considering a quadratic Lyapunov function in (17) and a bounded in amplitude $\boldsymbol{w}_{\xi}$ in (9) that satisfies $W_{\xi}=\{\boldsymbol{w}_{\xi}\in R^{q};\boldsymbol{w}_{\xi}^{\mathrm{T}}\boldsymbol{w}_{\xi}\le\delta_{\xi}^{-1}\}$, and the application of the well-known S-procedure, a sufficient condition to obtain a solution to **Problem 1** is achieved if the following relation is satisfied $\forall \boldsymbol{x}\in\varepsilon(\mathbf{P},\eta)$ and $\forall \boldsymbol{w}_{\mathrm{p}}\in W_{\mathrm{p}}$:

$$J(t)=\dot{V}(\boldsymbol{x})+\frac{1}{\gamma}\boldsymbol{z}^{\mathrm{T}}\boldsymbol{z}-\boldsymbol{w}_{\mathrm{p}}^{\mathrm{T}}\boldsymbol{w}_{\mathbf{p}}+\tau_1(\boldsymbol{x}^{\mathbf{T}}\mathbf{P}\boldsymbol{x}-\eta^{-1})+\tau_2(\delta_{\xi}^{-1}-\boldsymbol{w}_{\xi}^{\mathrm{T}}\boldsymbol{w}_{\xi})<0 \tag{23}$$

where $\tau_1>0$, $\tau_2>0$ and $\gamma>0$, $\mathbf{P}=\mathbf{P}^{\mathbf{T}}>\mathbf{0}$, $\boldsymbol{w}_{\mathrm{p}}$ is the energy bounded disturbance, and $\boldsymbol{w}_{\xi}$ is the amplitude bounded disturbance. One obtains:

$$\begin{aligned}&\int_0^T J(t)dt=\\&V(\boldsymbol{x}(T))-V(\boldsymbol{x}(0))+\frac{1}{\gamma}\int_0^T\boldsymbol{z}^{\mathrm{T}}\boldsymbol{z}dt-\int_0^T\boldsymbol{w}_{\mathbf{p}}^{\mathrm{T}}\boldsymbol{w}_{\mathbf{p}}dt+\tau_1\int_0^T(\boldsymbol{x}(t)^{\mathrm{T}}\mathbf{P}\boldsymbol{x}(t)-\eta^{-1})dt+\tau_2\int_0^T(\delta_{\xi}^{-1}-\boldsymbol{w}_{\xi}^{\mathrm{T}}\boldsymbol{w}_{\xi})dt<0\end{aligned} \tag{24}$$

and it is possible to conclude that:

1. If $\boldsymbol{w}_{\mathbf{p}}(t)=0$, relation (23) ensured that $\dot{V}(x)<0$ for any $\boldsymbol{x}$ such that $\boldsymbol{x}'\mathbf{P}\boldsymbol{x}>\eta^{-1}$ and for any $\boldsymbol{w}_{\xi}\in W_{\xi}$, which ensures that $\boldsymbol{x}(t)\to 0$ as $t\to\infty$, the trajectories of the saturated system (21) do not leave the set $\varepsilon(\mathbf{P},\eta)$.

2. For $\boldsymbol{w}_{\mathbf{p}}$ such that $\|\boldsymbol{w}_{\mathbf{p}}\|_2^2\le\delta^{-1}$ and $\boldsymbol{x}(0)\in\varepsilon(\mathbf{P},\beta)$, it follows that $V(\boldsymbol{x}(T))<V(\boldsymbol{x}(0))+\|\boldsymbol{w}_{\mathbf{p}}\|_2^2\le\beta^{-1}+\delta^{-1}\le\eta^{-1}$, $\forall T>0$, i.e. the trajectories of the system (21) are

confined in the set $\varepsilon(\mathbf{P},\eta)$.

3. Considering that $\boldsymbol{x}(0)=0$, in this case $\eta^{-1}=\delta^{-1}$ and the L_2-gain of the system is given by $1/\gamma$, i.e. $\|\boldsymbol{z}\|_2^2 < \gamma \|\boldsymbol{w}_\mathbf{p}\|_2^2$.

4. In the case of a non-null initial condition $\boldsymbol{x}(0)$, since $\beta^{-1}+\delta^{-1}=\eta^{-1}$ there is a trade-off between the size of the set of admissible conditions (given basically by β^{-1}), and the size of the admissible norm of the exogenous signal (given by δ^{-1}). In this case, for $T\to\infty, \|\boldsymbol{z}\|_2^2 < \gamma(\|\boldsymbol{w}_\mathbf{p}\|_2^2 + V(\boldsymbol{x}(0)))$; the finite L_2-gain from $\boldsymbol{w}_\mathbf{p}$ to $\boldsymbol{z}$ presents a bias term.

3.3 One-step controller schemes with regional stability guarantees

In this section, we provide some results to address the design problem of one-step controller, that is, the determination of matrices $\mathbf{A_c},\mathbf{B_c},\mathbf{C_c},\mathbf{D_c},\mathbf{D_{aw}}$ simultaneously with consideration of both amplitude bounded and energy bounded signals. Considering a simplified anti-windup controller in one-step method, the anti-windup output is only injected in the dynamics of $\boldsymbol{x}_\mathrm{c}$, hence $\mathbf{D}_{\mathrm{awy}}=0$. The following proposition is used to design the one-step controller.

Propositon1 If there exist symmetric positive define matrices $\mathbf{X}\in R^{n\times n}$, $\mathbf{Y}\in R^{n\times n}$, a positive definite diagonal matrix $\mathbf{S}\in R^{m\times m}$, matrices $\mathbf{Q}\in R^{n\times m}$, $\mathbf{L}\in R^{m\times n}$, $\mathbf{F}\in R^{n\times p}$, $\mathbf{W}\in R^{n\times n}$, $\mathbf{Z}\in R^{m\times n}$, $\mathbf{Z}_1\in R^{m\times n}$ and positive scalars γ, τ_1 and τ_2 such that the following conditions hold:

$$\begin{bmatrix} \mathbf{YA}_p^{\mathrm{T}} + \mathbf{A}_p\mathbf{Y} + \mathbf{B}_{pu}\mathbf{L} + \mathbf{L}^{\mathrm{T}}\mathbf{B}_{pu}^{\mathrm{T}} + \tau_1\mathbf{Y} & \mathbf{W} + \tau_1\mathbf{I} \\ * & \mathbf{A}_p^{\mathrm{T}}\mathbf{X} + \mathbf{XA}_p + \mathbf{C}_p^{\mathrm{T}}\mathbf{F}^{\mathbf{T}} + \mathbf{FC}_p + \tau_1\mathbf{X} \\ * & * \\ * & * \\ * & * \\ * & * \end{bmatrix}$$

$$\begin{bmatrix} \mathbf{B}_{pu}\mathbf{S} - \mathbf{Z}^{\mathrm{T}} - \mathbf{L}^{\mathrm{T}} & \mathbf{B}_{pw} & 0 & \mathbf{YC}_z^{\mathrm{T}} \\ \mathbf{Q} - \mathbf{Z}_1^{\mathrm{T}} - \mathbf{C}_p^{\mathbf{T}}\mathbf{D}_c^{\mathrm{T}} & \mathbf{XB}_w & 0 & \mathbf{C}_z^{\mathrm{T}} \\ -2\mathbf{S} & 0 & -\mathbf{D}_{c\xi} & 0 \\ * & -\mathbf{I} & 0 & 0 \\ * & * & -\tau_2\mathbf{I} & 0 \\ * & * & * & -\gamma\mathbf{I} \end{bmatrix} < 0 \tag{25}$$

$$\begin{bmatrix} \mathbf{Y} & \mathbf{I} & \mathbf{Z}_{(i)}^{\mathrm{T}} \\ \mathbf{I} & \mathbf{X} & \mathbf{Z}_{\mathbf{1}(i)}^{\mathrm{T}} \\ \mathbf{Z}_{(i)} & \mathbf{Z}_{\mathbf{1}(i)} & \delta u_{0(i)}^2 \end{bmatrix} \geq 0, i = 1, \ldots, m \tag{26}$$

$$-\tau_1\delta^{-1} + \tau_2\delta_\xi^{-1} < 0 \tag{27}$$

then the controller (20) with

$$\begin{aligned} &\mathbf{D}_{awx} = \mathbf{U}^{-1}(\mathbf{Q} - \mathbf{XB}_{pu}\mathbf{S})\mathbf{S}^{-1} \\ &\mathbf{D}_c = \mathbf{D}_c \\ &\mathbf{C}_c = (\mathbf{L} - \mathbf{D}_c\mathbf{C}_p\mathbf{Y})(\mathbf{V}^{\mathrm{T}})^{-1} \\ &\mathbf{B}_c = \mathbf{U}^{-1}(\mathbf{F} - \mathbf{XB}_{pu}\mathbf{D}_c) \\ &\mathbf{A}_c = \mathbf{U}^{-1}(\mathbf{W}^{\mathrm{T}} - (\mathbf{A}_p + \mathbf{B}_{pu}\mathbf{D}_c\mathbf{C}_p)^{\mathrm{T}} - \mathbf{XA}_p\mathbf{Y} - \mathbf{XB}_{pu}\mathbf{L} - \mathbf{UB}_c\mathbf{C}_p\mathbf{Y})(\mathbf{V}^{\mathrm{T}})^{-1} \end{aligned} \tag{28}$$

is such that the condition (23) for **Problem 1** is verified.

Proof：The relation (23) is verified if

$$\dot{V}(\mathbf{x}) + \frac{1}{\gamma}\mathbf{z}^{\mathrm{T}}\mathbf{z} - \mathbf{w}_p{}^{\mathrm{T}}\mathbf{w}_p + \tau_1\mathbf{x}^{\mathrm{T}}\mathbf{P}\mathbf{x} - \tau_2\mathbf{w}_\xi^{\mathrm{T}}\mathbf{w}_\xi < 0 \tag{29}$$

and

$$-\tau_1\eta^{-1} + \tau_2\delta_\xi^{-1} < 0 \tag{30}$$

are satisfied.

Consider the quadratic Lyapunov function $V(\boldsymbol{x})$ defined in (17) and the sector nonlinearity $\phi(\bar{\boldsymbol{y}}_c)$ satisfies the inequality (16), use this sector condition into (29), which implies that

$$\dot{V}(\boldsymbol{x}) + \frac{1}{\gamma}\mathbf{z}^{\mathrm{T}}\mathbf{z} - \boldsymbol{w}_p^{\mathrm{T}}\boldsymbol{w}_p + \tau_1\mathbf{x}^{\mathrm{T}}\mathbf{P}\mathbf{x} - \tau_2\boldsymbol{w}_\xi^{\mathrm{T}}\boldsymbol{w}_\xi - 2\phi(\bar{\boldsymbol{y}}_c)^{\mathrm{T}}\mathbf{T}(\phi(\bar{\boldsymbol{y}}_c) + \bar{\boldsymbol{y}}_c + \mathbf{G}\boldsymbol{x}) < 0 \tag{31}$$

The right term of the inequality (31) reads

$$\begin{bmatrix} x \\ \phi(\bar{y}_c) \\ w_p \\ w_\xi \\ z \end{bmatrix}^T \begin{bmatrix} A^TP+PA+\tau_1 P & PB-G^TS^{-1}-C^TS^{-1} & PB_w & PB_\xi & 0 \\ * & -2S^{-1}-S^{-1}D-DS^{-1} & -S^{-1}D_w & -S^{-1}D_\xi & 0 \\ * & * & -I & 0 & 0 \\ * & * & * & -\tau_2 I & 0 \\ * & * & * & * & \frac{1}{\gamma}I \end{bmatrix} \begin{bmatrix} x \\ \phi(\bar{y}_c) \\ w_p \\ w_\xi \\ z \end{bmatrix} < 0 \tag{32}$$

where $S = T^{-1}$. Then follow the same lines as that one of Proposition3.20 in reference [13] or proof process of theorem 1 in reference [14], LMI (25) can be proved. The satisfaction of relation (26) ensures that $\varepsilon(P,\eta) \subset S(|\bar{y}_c - y_g|, u_0)$ according to (18) to obtain the regional stability.

3.4 Traditional anti-windup controller schemes with regional stability guarantees

The controller structure shown in Fig.1 shows there can be a separation between the controller and the anti-windup compensator. The controller is designed as an unconstrained controller, and the anti-windup compensator is driven by the difference between the constrained and unconstrained control signals [13].

Proposition 2: If there exists a symmetric positive define matrix $Q \in R^{(n+n_c)\times(n+n_c)}$, positive definite diagonal matrices $Z \in R^{m\times n}$, $E \in R^{(n_c+m)\times m}$ and positive scalars γ, τ_1 and τ_2 such that the following conditions hold:

$$\begin{bmatrix} QA^T+AQ+\tau_1 Q & B_1S+B_2E-QC^T-Z^T & B_\xi & B_w & QC_z^T \\ * & -2S-\begin{bmatrix} 0 \\ I_m \end{bmatrix}^T E-E^T\begin{bmatrix} 0 \\ I_m \end{bmatrix} & -D_\xi & 0 & 0 \\ * & * & -\tau_2 I & 0 & 0 \\ * & * & * & -I & 0 \\ * & * & * & * & -\gamma I \end{bmatrix} < 0 \tag{33}$$

$$\begin{bmatrix} Q & Z_{(i)}^T \\ * & \delta u_{0(i)}^2 \end{bmatrix} \geq 0, i = 1\cdots m \tag{34}$$

$$-\tau_1\eta^{-1}+\tau_2\delta_\xi^{-1} < 0 \tag{35}$$

then the compensator (20) with $D_{aw} = ES^{-1}$, is such that the condition (23) for **Problem 1** is verified.

Proof: By pre- and post-multiplying (32) respectively by $\mathrm{diag}\begin{bmatrix}\mathbf{Q} & \mathbf{S} & \mathbf{I} & \mathbf{I} & 1/\gamma\end{bmatrix}$ with $\mathbf{P}=\mathbf{Q}^{-1}$, one obtains

$$\begin{bmatrix} \mathbf{QA}^{\mathrm{T}}+\mathbf{AQ}+\tau_1\mathbf{Q} & \mathbf{BS}-\mathbf{QG}^{\mathrm{T}}-\mathbf{QC}^{\mathrm{T}} & \mathbf{B}_{\xi} & \mathbf{B}_{w} & \mathbf{QC}_{z}^{\mathrm{T}} \\ * & -2\mathbf{S}-\mathbf{DS}-\mathbf{SD}^{\mathrm{T}} & -\mathbf{D}_{c\xi} & \mathbf{0} & \mathbf{0} \\ * & * & -\tau_2\mathbf{I} & \mathbf{0} & \mathbf{0} \\ * & * & * & -\mathbf{I} & \mathbf{0} \\ * & * & * & * & -\gamma\mathbf{I} \end{bmatrix} < 0 \tag{36}$$

Considering the change of variables $\mathbf{Z}=\mathbf{GQ}$, $\mathbf{E}=\mathbf{D}_{\mathbf{aw}}\mathbf{S}$, $\mathbf{B}=\begin{bmatrix}\mathbf{B}_1+\mathbf{B}_2\mathbf{D}_{\mathbf{aw}}\end{bmatrix}$ and $\mathbf{D}=\begin{bmatrix}\mathbf{0} & \mathbf{I}_{\mathbf{m}}\end{bmatrix}\mathbf{D}_{\mathbf{aw}}$, one gets LMI (34). By pre- and post-multiplying (18) with $\mathrm{diag}[\mathbf{Q} \quad \mathbf{I}]$, one gets LMI (36).

4. Application to a multi-vectored propeller airship model

4.1 Model introduction

An airship with a diameter of 6 m and a volume of 70 m^3 is shown in Fig.2. The airship is finless, and equipped with four vectored propellers, and the equipment tank is suspended under its body to increase pitch stability. Each vectored propeller can change its thrust amplitude and direction independently. Hence there are eight control degrees-of-freedom; the vectored thrusters have unsymmetrical saturation in that the thrust can be varied between zero and a maximum thrust value.

Fig. 2 Overall structure of the airship

The body frame is established as shown in Fig.3. The *x*-axis of the body-fixed frame is coincident with

one of the four thrusters. The vectored angle of each propeller is denoted by $\mu_i \in (-\pi, \pi), i = 1,2,3,4$, and the generated force is represented by $f_i \in (0, 20N)$, $i = 1,2,3,4$. In the vectored-rotation plane, each vectored thrust is decomposed into two orthogonal forces f_{iH} and f_{iV}. The pair f_{iH} and f_{iV} can then be resolved into the body-fixed frame along the *x*-, *y*-, and *z*-axes [25] so that

$$\begin{aligned}
F_{Tx} &= \boldsymbol{f_2}\sin(\mu_2) - \boldsymbol{f_4}\sin(\mu_4) \\
F_{Ty} &= -\boldsymbol{f_1}\sin(\mu_1) + \boldsymbol{f_3}\sin(\mu_3) \\
F_{Tz} &= \boldsymbol{f_1}\cos(\mu_1) + \boldsymbol{f_2}\cos(\mu_2) + \boldsymbol{f_3}\cos(\mu_3) + \boldsymbol{f_4}\cos(\mu_4) \\
M_{Tx} &= (-\boldsymbol{f_2}\cos(\mu_2) + \boldsymbol{f_4}\cos(\mu_4))R_p \\
M_{Ty} &= (\boldsymbol{f_1}\cos(\mu_1) - \boldsymbol{f_3}\cos(\mu_3))R_p \\
M_{Tz} &= -(\boldsymbol{f_1}\sin(\mu_1) + \boldsymbol{f_2}\sin(\mu_2) + \boldsymbol{f_3}\sin(\mu_3) + \boldsymbol{f_4}\sin(\mu_4))R_p
\end{aligned} \tag{37}$$

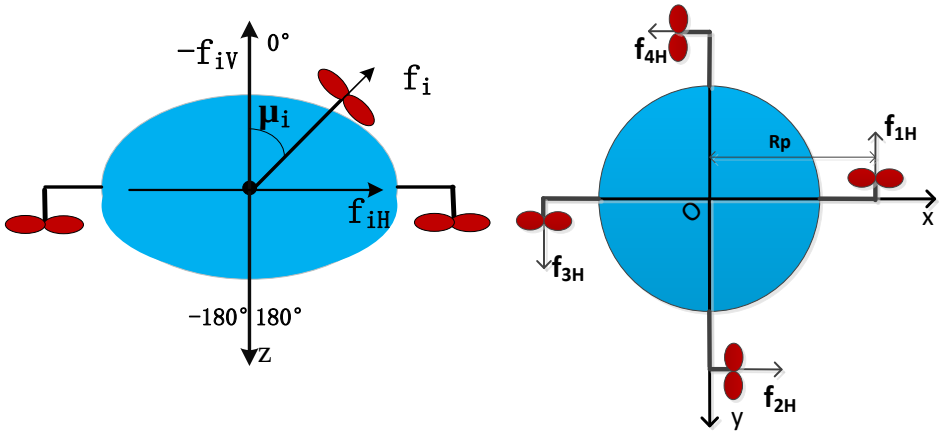

(a)Side view of the airship (b)Top view of the airship

Fig.3 Decomposition of the thrusts in the body-fixed frame

The dynamics of this vehicle are similar to those of a conventional airship. External forces and moments are induced by gravity, buoyancy, fluid inertia force, aerodynamics, and thrusters. Through force analysis, the following dynamics equation can be constructed in the body-fixed frame [25]:

$$\mathbf{M}\left[\dot{u}\ \dot{v}\ \dot{w}\ \dot{p}\ \dot{q}\ \dot{r}\right]^{\mathrm{T}} = \mathbf{F_T} + \mathbf{F_{GB}} + \mathbf{F_A} + \mathbf{F_I} \tag{38}$$

where $\mathbf{M}$ is the mass matrix; $\dot{u}, \dot{v}, \dot{w}$ denote linear accelerations; $\dot{p}, \dot{q}, \dot{r}$ represent the angular accelerations around the body frame; and the right-hand side of the equation corresponds to external forces and moments, including gravity and buoyancy $\boldsymbol{F_{GB}}$, aerodynamic force $\boldsymbol{F_A}$, coriolis force $\boldsymbol{F_I}$,

and vectored thrust $\boldsymbol{F_T}$.

4.2 Model linearization

The vehicle is in trimmed in forward flight with a longitudinal flight speed, a linear model can be obtained from linearization. Before linearization, the aerodynamic coefficients given in [25] were fitted as a function of flow angle of attack α in the approximated linear area about the trim point, hence we obtain $C_H = c_1 + b_1\alpha + a_1\alpha^2$, $C_Z = c_2 + b_2\alpha + a_2\alpha^2$ and $C_M = c_3 + b_3\alpha + a_3\alpha^2 - C_{Mq}$, where C_{Mq} is the pitch damping coefficient and $-30^o < \alpha < 30^o$.

Because of the symmetric shape of the vehicle and the symmetric flight condition, the linear model can be decoupled into longitudinal and lateral models. The obtained longitudinal linear model is:

$$\mathbf{M}_{\text{lon}}\dot{\boldsymbol{x}}_{\boldsymbol{p}} = \mathbf{A}_{\text{lon}}\boldsymbol{x}_{\boldsymbol{p}} + \mathbf{B}_{\text{lon}}\boldsymbol{u} \tag{39}$$

with $\boldsymbol{x_p} = [u, w, q, \theta]^{\mathrm{T}}$, $\boldsymbol{u} = [\,f_1 \quad f_2 \quad f_3 \quad f_4 \quad \mu_1 \quad \mu_2 \quad \mu_3 \quad \mu_4\,]^{\mathrm{T}}$ and

$$\mathbf{M}_{\text{lon}} = \begin{bmatrix} m+m_{11} & 0 & mz_G & 0 \\ 0 & m+m_{33} & 0 & 0 \\ mz_G & 0 & i_y+m_{55} & 0 \\ 0 & 0 & 0 & 1 \end{bmatrix}$$

$$\mathbf{A}_{\text{lon}} = \begin{bmatrix} \rho s_{ref} C_{H0} c\varphi_0 u_0 & \rho s_{ref} a_1 \alpha_0 c\varphi_0 u_0 & 0 & 0 \\ \rho s_{ref} C_{Z0} u_0 & \rho s_{ref} a_2 \alpha_0 u_0 & (m+m_{11})u_0 & 0 \\ \rho s_{ref} l_{ref} C_{M0} c(\varphi_0) u_0 & \rho s_{ref} l_{ref} a_3 \alpha_0 c\varphi_0 u_0 & -C_{Mq} & -Gz_G \cos(\theta_0) \\ 0 & 0 & 1 & 0 \end{bmatrix}$$

$$\mathbf{B}_{\text{lon}} = \begin{bmatrix} 0 & \mathrm{s}\,\mu_{20} & 0 & -\mathrm{s}\,\mu_{40} & 0 & f_{20}\,\mathrm{c}\,\mu_{20} & 0 & -f_{40}\,\mathrm{c}\,\mu_{40} \\ -\mathrm{c}\,\mu_{10} & -\mathrm{c}\,\mu_{20} & -\mathrm{c}\,\mu_{30} & -\mathrm{c}\,\mu_{40} & f_{10}\,\mathrm{s}\,\mu_{10} & f_{20}\,\mathrm{s}\,\mu_{20} & f_{30}\,\mathrm{s}\,\mu_{30} & f_{40}\mathrm{s}\mu_{40} \\ R_p\,\mathrm{c}\,\mu_{10} & 0 & -R_p\,\mathrm{c}\,\mu_{30} & 0 & -R_p f_{10}\,\mathrm{s}\,\mu_{10} & 0 & R_p f_{30}\,\mathrm{s}\,\mu_{30} & 0 \\ 0 & 0 & 0 & 0 & 0 & 0 & 0 & 0 \end{bmatrix}$$

where s represents the triangular sine function, c represents the triangular cosine function and subscript 0 represents the trim value. All the other parameter definitions and values can be found in [25].

Given $u_0 = 4.118m/\mathrm{s}$ with trimmed control input $\boldsymbol{u}_{trim} = [0 \;\; 10 \;\; 0 \;\; 10 \;\; 0 \;\; \frac{1}{2}\pi \;\; 0 \;\; -\frac{1}{2}\pi]^{\mathrm{T}}$, the obtained linear model is given

$$\dot{\boldsymbol{x}}_p = \mathbf{A}_{\mathbf{p}}\boldsymbol{x}_p + \mathbf{B}_{\mathbf{pu}}\boldsymbol{u} \tag{40}$$

$$\mathbf{A}_{\mathbf{p}} = \begin{bmatrix} -0.2482 & -0.0230 & 0 & 11.7399 \\ 0 & -0.0081 & 3.2095 & 0 \\ 0.0811 & 0.0136 & 0 & -6.9445 \\ 0 & 0 & 1.000 & 0 \end{bmatrix}$$

$$\mathbf{B}_{\mathbf{pu}} = \begin{bmatrix} -0.0224 & 0.0270 & 0.0224 & 0.0270 & 0 & 0.0000 & 0 & -0.0000 \\ -0.0090 & -0.0000 & -0.0090 & -0.0000 & 0 & 0.0901 & 0 & -0.0901 \\ 0.0133 & -0.0088 & -0.0133 & -0.0088 & 0 & -0.0000 & 0 & 0.0000 \\ 0 & 0 & 0 & 0 & 0 & 0 & 0 & 0 \end{bmatrix}$$

The linear model of the airship in equation (40) is open-loop stable, the eigenvalues are $-0.0684 \pm 2.6232i$, -0.1113 and -0.0082. The complex pair represents the lightly damped oscillation mode in pitch motion, the other two real roots represent the surge mode in longitudinal and vertical velocity respectively. The upper limits of the actuator around the trim point are $\mathbf{a} = \mathrm{diag}\left[20 \;\; 10 \;\; 20 \;\; 10 \;\; \pi \;\; \frac{1}{2}\pi \;\; \pi \;\; \frac{3}{2}\pi\right]$, and the lower limits are $\mathbf{b} = \mathrm{diag}\left[0 \;\; -10 \;\; 0 \;\; -10 \;\; -\pi \;\; -\frac{3}{2}\pi \;\; -\pi \;\; -\frac{1}{2}\pi\right]$. The new variable $\bar{\boldsymbol{y}}_c = \boldsymbol{y}_c - \frac{\mathbf{a}+\mathbf{b}}{\mathbf{2}}\boldsymbol{\xi}$ is introduced here, by using the variable transformation, then the unsymmetrical constrains are transformed into the symmetrical constraints, $\boldsymbol{u}_0 = \frac{\mathbf{a}-\mathbf{b}}{\mathbf{2}}\boldsymbol{\xi} = \left[10 \;\; 10 \;\; 10 \;\; 10 \;\; \pi \;\; \pi \;\; \pi \;\; \pi\right]^{\mathrm{T}}$ as described in equation (8).

4.3 Results and discussion

The controller problems of Proposition 1 and 2 were solved using the YALMIP toolbox [13]. Regions of stability in a 2-D plane for each pair of variables are presented; the actuator saturation depth was calculated to evaluate the reliability of the controller; control performances in terms of anti-windup ability and disturbance rejection ability were studied to validate the controller.

4.3.1 Controller solutions

Three controllers were designed and tested on the airship model. The first is an unconstrained dynamic output feedback controller obtained from an LQG formulation, and it was designed based on the unsaturated linear system model. The second is a one-step controller in which a dynamic output feedback controller with an anti-windup compensator were calculated together by solving the LMIs (25), (26) and (27). The third is an anti-windup compensator obtained by solving LMIs (33), (34) and (35) with the unconstrained linear LQG controller. Even though the linear model is open-loop stable, we still focus on a robust local stabilization approach for relaxing open-loop stability assumptions and by using the local stability condition, a solution that satisfies the performance criteria in our interested region of stability is obtained quickly. The inequalities (25) and (33) are BMIs, if δ and τ_1 are decision variables and LMIs if these are fixed *a priori*. The three controllers solve a MIMO problem, so the allocation of multi-vectored thrusters is directly obtained in the controller design.

The LQG controller has

$$\mathbf{A_c} = \begin{bmatrix} -10.5492 & 7.1174 & 7.9906 & 7.5164 \\ 0.0082 & -7.7106 & 0.2725 & 1.7432 \\ 3.1969 & -4.9255 & -7.7370 & -5.0682 \\ -2.0299 & -0.0731 & 1.8586 & -1.8492 \end{bmatrix}$$

$$\mathbf{B_c} = \begin{bmatrix} 6.7980 & -0.2582 & -1.9747 & 2.0299 \\ -0.2582 & 4.1252 & 1.4361 & 0.0731 \\ -1.9747 & 1.4361 & 3.8659 & -0.8586 \\ 2.0299 & 0.0731 & -0.8586 & 1.8492 \end{bmatrix}$$

$$\mathbf{C}_c = \begin{bmatrix} 13.7044 & 100.5864 & -63.2829 & -76.7917 \\ -64.9159 & 39.4622 & -22.0105 & -19.4785 \\ 13.8015 & 292.9451 & 228.3942 & -123.0165 \\ -64.9159 & 39.4622 & -22.0105 & -19.4785 \\ 0 & 0 & 0 & 0 \\ -0.0138 & -0.1970 & -0.0826 & 0.1 \\ 0 & 0 & 0 & 0 \\ 0.0138 & 0.1970 & 0.0826 & -0.1000 \end{bmatrix}$$

$$\mathbf{D}_c = \mathbf{0}_{8\times 4}$$

The one-step controller and traditional anti-windup controller have different solutions for different given δ and τ_1. The best obtained solutions of the two kinds of anti-windup controllers are given below. The optimal objectives γ, τ_2 and the tracking ability of step response are used to evaluate the control performance.

For the one-step controller, for given values δ=1×10^{-7} and $\tau_1 = 0.01$, the values obtained are $\tau_2 = 3425$ and $\gamma = 88$, with controller matrices calculated as:

$$\mathbf{A}_c = 1\times 10^4 \begin{bmatrix} -0.0604 & -0.0000 & 0.0000 & 0.0000 \\ -1.7013 & -0.4228 & -0.0135 & 1.3593 \\ 0.0532 & -0.0000 & -0.0014 & -0.0010 \\ -0.0005 & 0.0000 & 0.0004 & -0.0001 \end{bmatrix}$$

$$\mathbf{B}_c = 1\times 10^5 \begin{bmatrix} -6.7361 & 0.0001 & -0.0919 & -0.0664 \\ 0.0001 & -1.1261 & -3.6522 & 0.0000 \\ -0.0919 & -3.6522 & -1.1444 & 6.7358 \\ -0.0664 & 0.0000 & 6.7358 & -1.1445 \end{bmatrix}$$

$$\mathbf{C}_c = \begin{bmatrix} -0.0418 & -0.0103 & 0.0016 & 0.0333 \\ 0.1309 & 0.0003 & -0.0001 & -0.0011 \\ -0.0412 & -0.0103 & -0.0023 & 0.0330 \\ 0.1309 & 0.0003 & -0.0001 & -0.0011 \\ 0 & 0 & 0 & 0 \\ 0.4125 & 0.1025 & 0.0033 & -0.3295 \\ 0 & 0 & 0 & 0 \\ -0.4125 & -0.1025 & -0.0033 & 0.3295 \end{bmatrix}$$

$$D_c = 0_{8\times 4}$$

$$\mathbf{D}_{\mathbf{awx}} = 1\times10^{4}\begin{bmatrix} 0.0028 & -0.0031 & -0.0028 & -0.0031 & 0 & -0.0000 & 0 & 0.0000 \\ 0.2040 & 0.0000 & 0.2040 & 0.0000 & 0 & -2.0419 & 0 & 2.0419 \\ -0.3309 & 0.1994 & 0.3309 & 0.1994 & 0 & -0.0000 & 0 & 0.0000 \\ -0.0000 & -0.0000 & -0.0000 & -0.0000 & 0 & 0.0001 & 0 & -0.0001 \end{bmatrix}$$

For the traditional anti-windup compensator, with the above unconstrained LQG controller, with given values δ=4 and $\tau_1 = 0.01$, the obtained values are $\tau_2 = 0.00088$ and γ=5.6×10^{7}, and the matrices of the calculated compensator are:

$$\mathbf{D}_{\mathbf{awx}} = \begin{bmatrix} 0.0041 & 0.1499 & -1.0518 & 0.1499 & 0 & -0.1240 & 0 & 0.1104 \\ 0.2032 & -0.1088 & 2.8750 & -0.1088 & 0 & 0.2685 & 0 & -0.1906 \\ -0.0494 & -0.2502 & 1.6688 & -0.2502 & 0 & 0.0440 & 0 & -0.0400 \\ -0.0677 & -0.2905 & 1.0081 & -0.2905 & 0 & 0.0570 & 0 & -0.0476 \end{bmatrix}$$

$$\mathbf{D}_{\mathbf{awy}} = \begin{bmatrix} 1.0000 & -0.2719 & -6.6852 & -0.2719 & 0 & -1.9441 & 0 & 2.1157 \\ -0.6444 & 1.0000 & 4.9532 & 0.8360 & 0 & -1.0035 & 0 & 0.9284 \\ 1.1955 & -1.0029 & 1.0000 & -1.0029 & 0 & -1.5655 & 0 & 1.7560 \\ -0.6444 & 0.8360 & 4.9532 & 1.0000 & 0 & -1.0035 & 0 & 0.9284 \\ 0 & 0 & 0 & 0 & 1.0000 & 0 & 0 & 0 \\ 0.2273 & 0.0571 & 1.2012 & 0.0571 & 0 & 1.0000 & 0 & 1.7735 \\ 0 & 0 & 0 & 0 & 0 & 0 & 1.0000 & 0 \\ -0.2201 & -0.0492 & -1.1941 & -0.0492 & 0 & 1.4705 & 0 & 1.0000 \end{bmatrix}$$

From the above results we can conclude:

1) The one-step anti-windup controller has good disturbance rejection ability with a lower value of γ as compared with that of the traditional anti-windup compensator.

2) The gains in the obtained controller coefficient matrix and anti-windup coefficient matrix of one-step methods are very high. Clearly, these are not suitable for implementation. For the given linear controller, the traditional anti-windup compensator methods gives smaller anti-windup coefficient matrices that are more applicable for a real system.

3）From the calculated matrices *P* and *G*, the region of stability represented by ellipsoid set (17) and the allowance state of saturated system represented by polyhedral set (15) can be determined. However it is difficult to describe accurately in a graph because of the multi-variable (4 state variables) coupled

relationship. Fig.4 gives an approximation of the region of stability for each longitudinal variable pair in a 2-D plane.

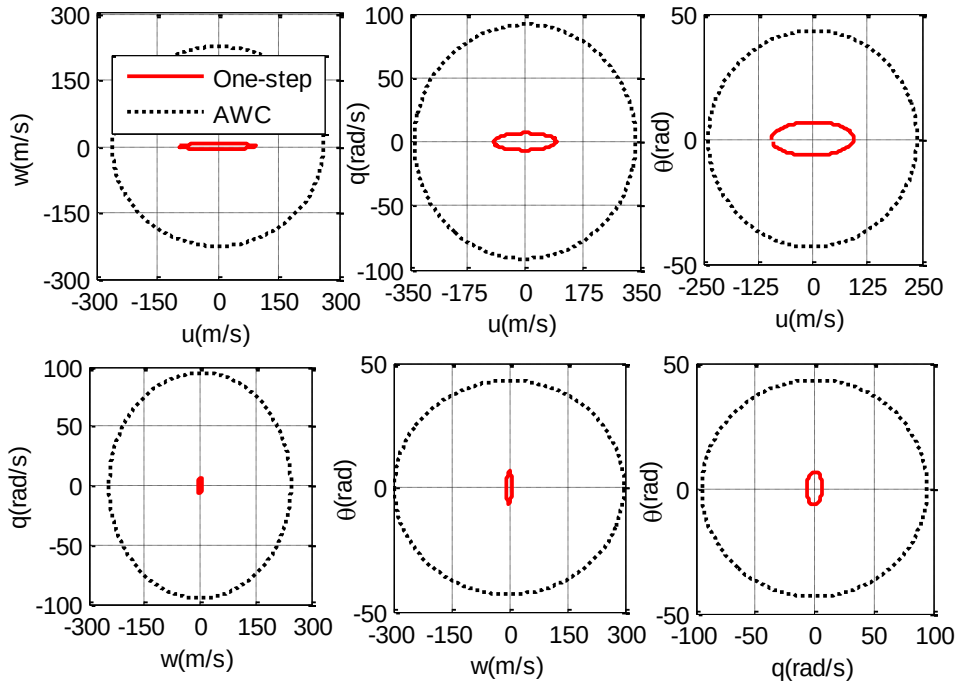

Fig.4 Regions of stability in 2-D plane of two methods

From Fig.4 we can see that the region of stability of the one-step method is very small compared with that of the traditional anti-windup compensator method. This is because the one-step method simultaneously takes into account performance and the safe domain of operation. In order to obtain a minimum γ, the resulting region of stability is very small. For the anti-windup compensator, the performance is mainly controlled by the linear controller and so the region of stability is enlarged by the compensator.

4.3.2 Actuator saturation depth

In this section we consider the difference of the controller output with real control input, which in this

paper we call the *actuator saturation depth*. This saturation depth is an excess control demand above the saturation limits of each actuator calculated from controller. High level of actuator saturation depth makes the controller difficult to recover from the saturation state, and such a system will be uncontrolled. Although it is not a quantitative criteria, actuator saturation depth can be taken as an evaluation of the reliability of a controller. From Figs 5 - 8 we can see that the control saturation depth of the one-step method is relatively large compared with that of the AWC method. Furthermore, as shown in Fig.5, saturation occurred during the whole control process for the one-step controller so this decreases the control reliability. That is because the one-step controller takes more constraints into consideration in controller design, so it is more conservative. The control saturation depth of the AWC method are small, and only occurred at the beginning as shown in Fig.7, which means this controller can withdraw from the saturation quickly and it makes the control system more reliable.

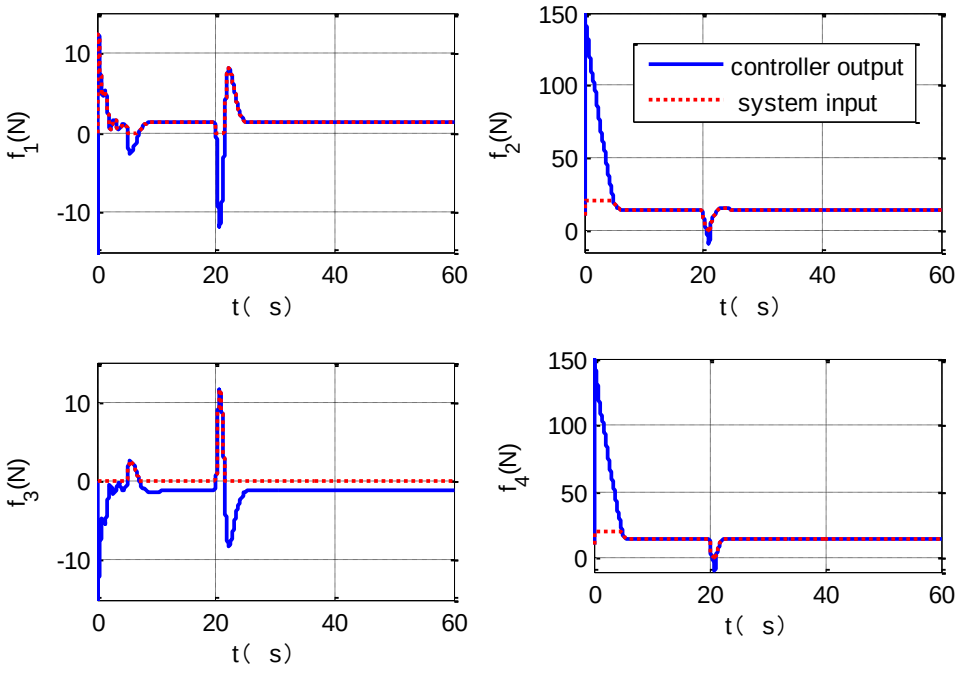

Fig.5 Controller output force and system input in one-step method

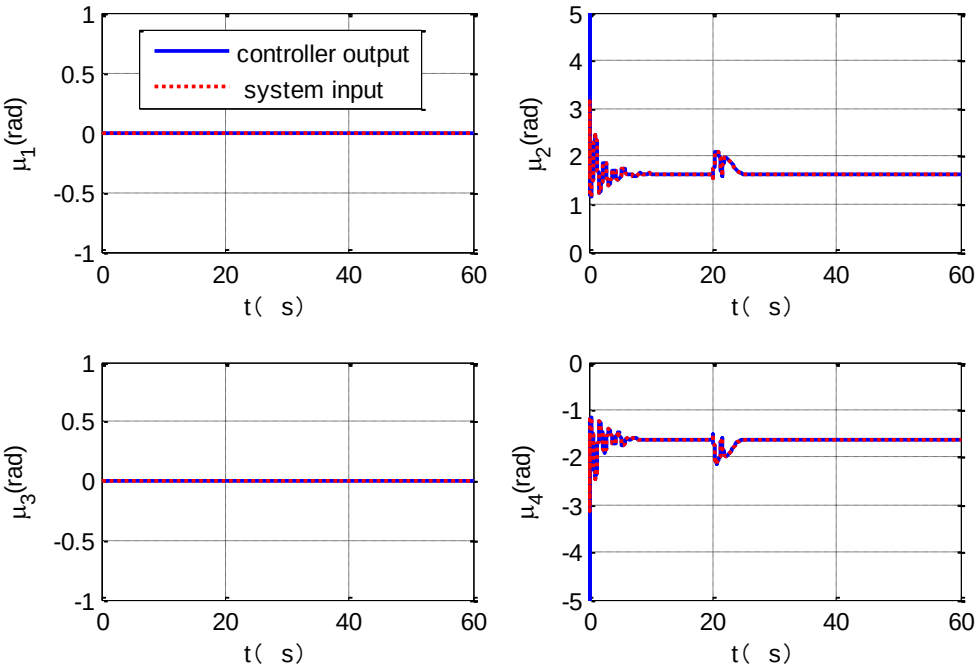

Fig.6 Controller output vectored angle and system input in one-step method

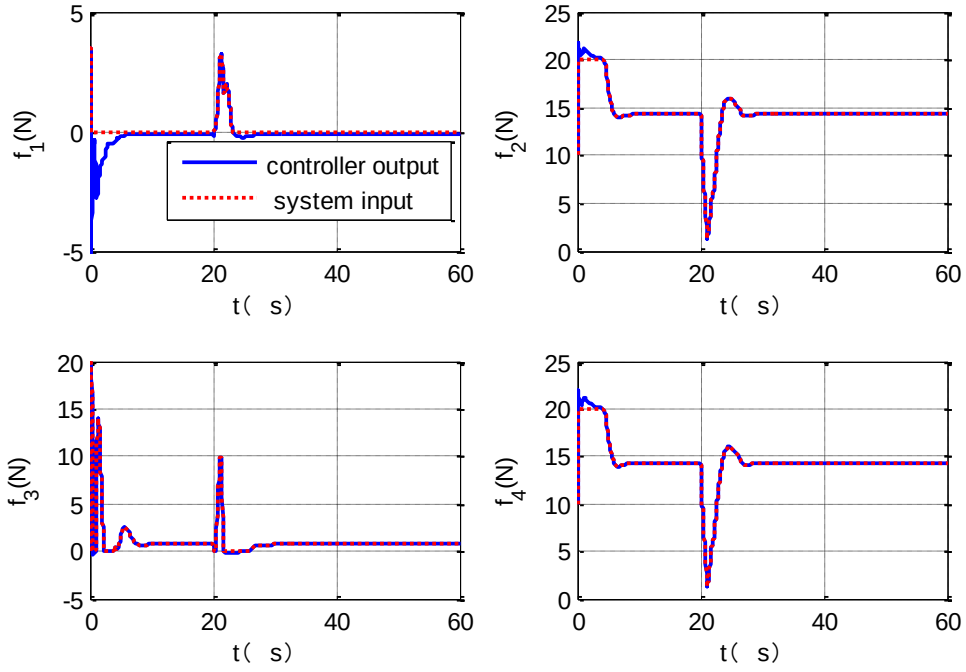

Fig.7 Controller output force and system input in AWC method

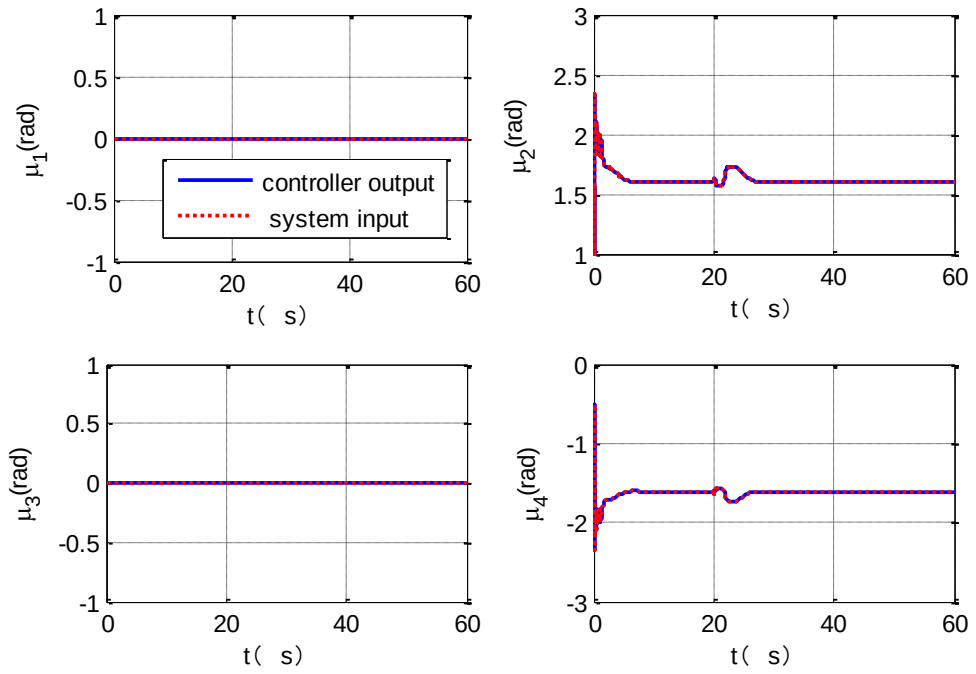

Fig.8 Controller output vectored angle and system input in AWC method

4.3.3 Performance of the controller

To validate the controllers, three simulation cases were implemented: the first two are based on the linear model, and the last is based on the nonlinear model. The first case is based on the linear model with the velocity tracking of a 1m/s step demand at t=0 s and a gust with amplitude of $0.5m/s$ at t = 20 s. In this situation actuator saturation occurs (Fig.9-Fig.11). The second case is based on the linear model with the velocity tracking of a 0.2m/s step demand at t=0 s and a gust with amplitude of $0.2m/s$ at t = 20 s, in this situation no actuator saturation occurs (Fig.12-Fig.14). The third case is based on the nonlinear model with the same condition as in the first case (Fig.15-Fig.17).

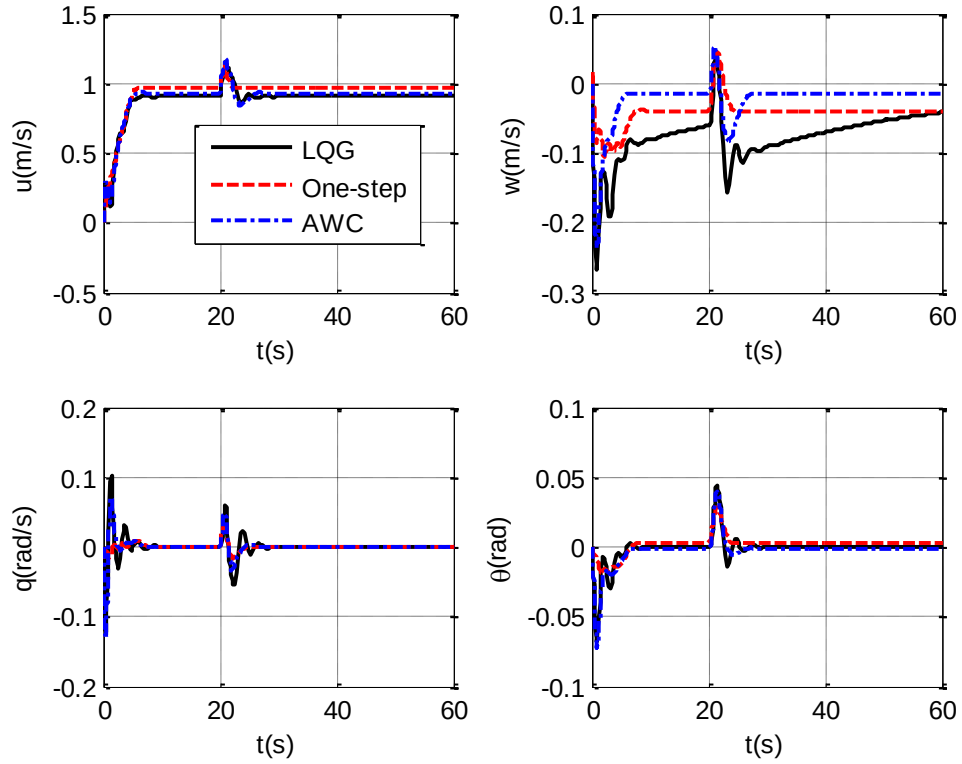

Fig.9 Time evolution of state (First case with saturation)

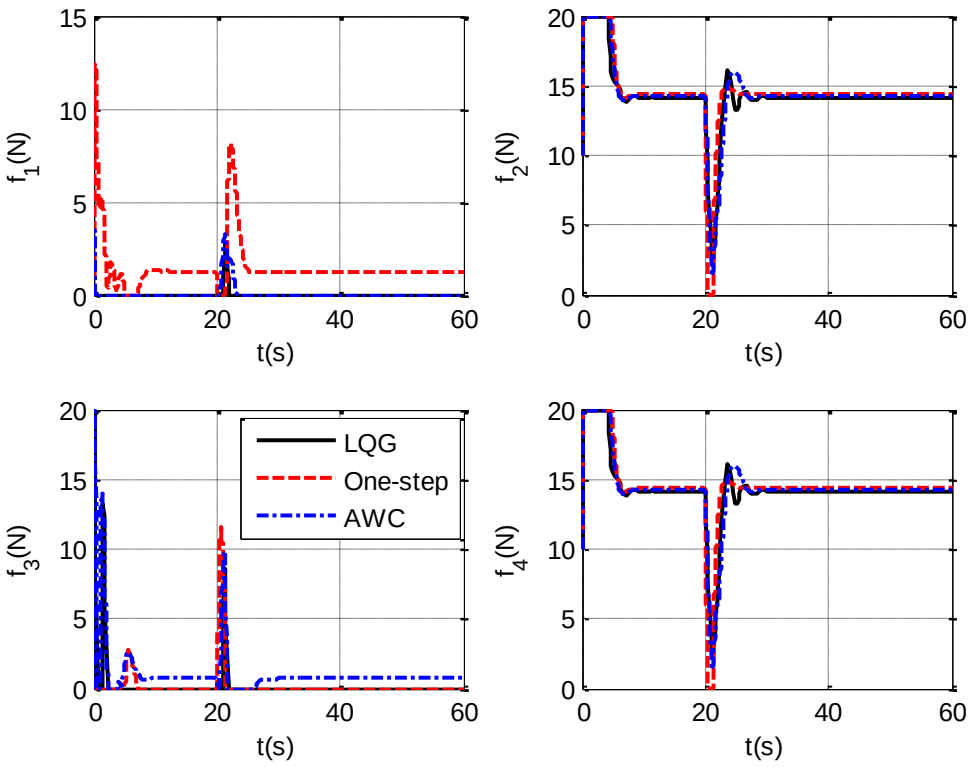

Fig.10 Time evolution of force (First case with saturation)

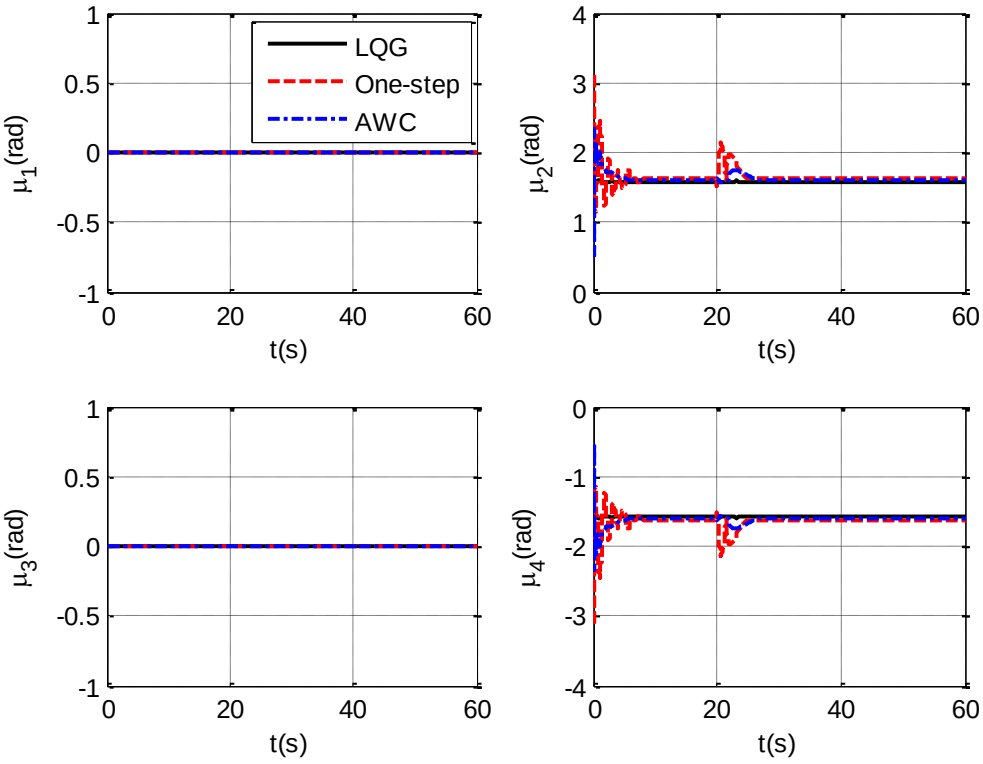

Fig.11 Time evolution of vectored angle (First case with saturation)

From Fig. 10 we see that both propellers 1 and 3 vary only their thrusts to suppress the disturbance generated during transient process. Propellers 2 and 4 were used for forward velocity tracking, so they have the same force amplitude, but with opposite direction as shown in Fig.11. The saturation occurred for both the velocity tracking and the disturbance rejection.

All three control systems converge to the trim position after a transient period when saturations are active as shown in Fig.9. The linear LQG controller presents rather poor performance regarding disturbance rejection and its input presents a slowly damped oscillation. Both anti-windup controllers have better tracking results and less input oscillation compared with the linear controller. The one-step method has better disturbance rejection and the transient states are smooth. The AWC method has more oscillation in the initial tracking phase and the disturbance rejection phase. It is because when the condition changed, the nominal linear controller responds rapidly, then the anti-windup compensator

followed if saturation occurred, so the traditional anti-windup method has more sensitivity to external disturbances.

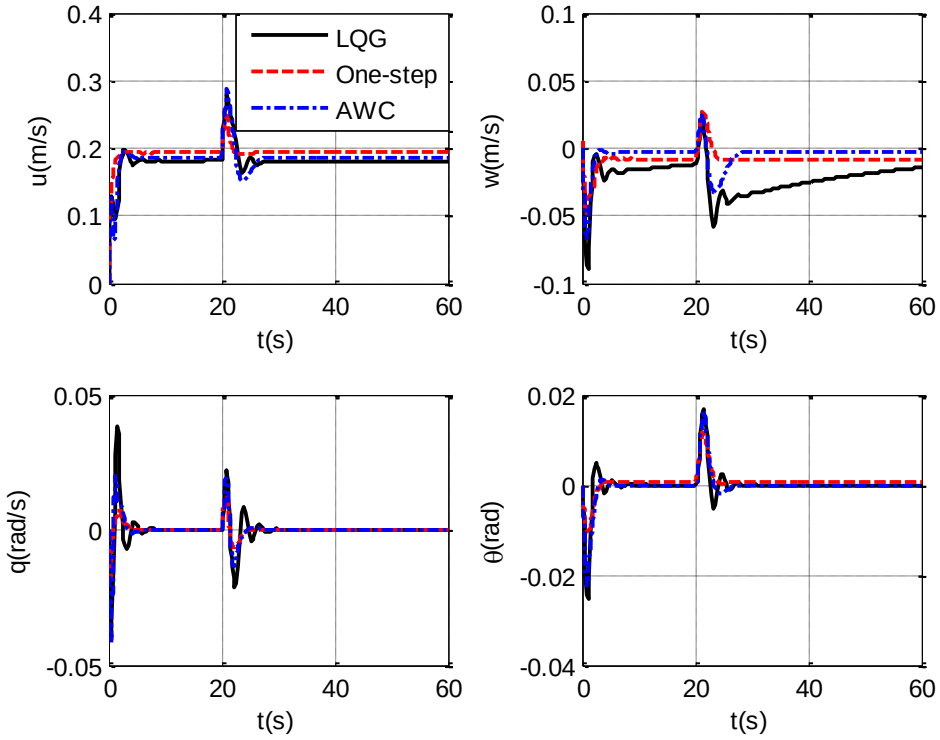

Fig.12 Time evolution of state (Second case without saturation)

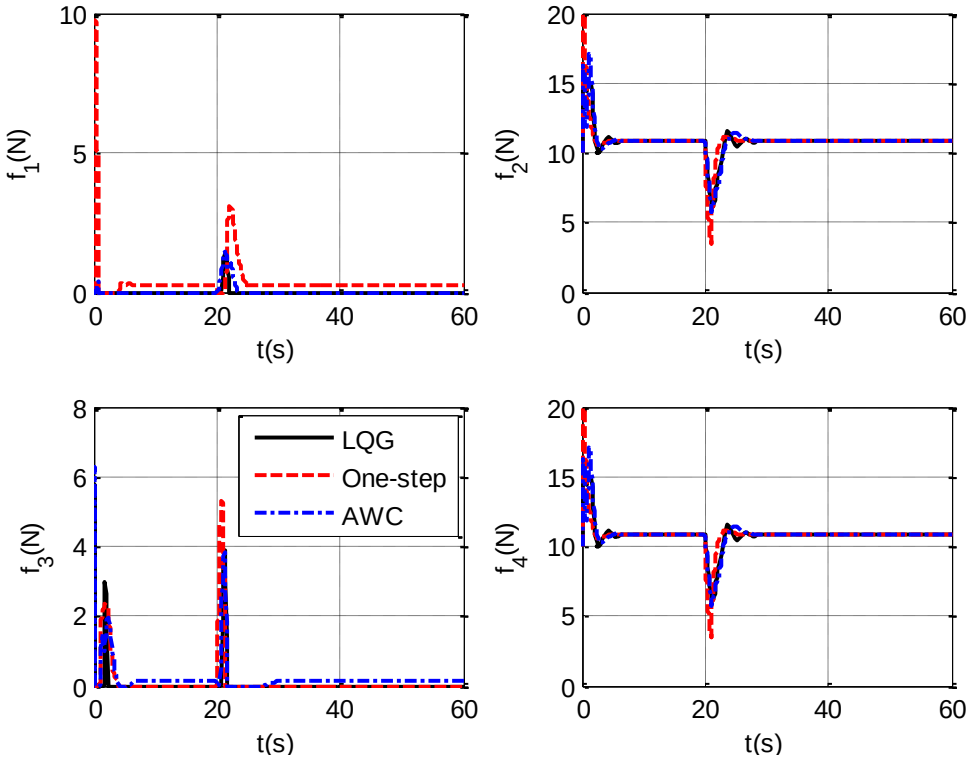

Fig.13 Time evolution of force (Second case without saturation)

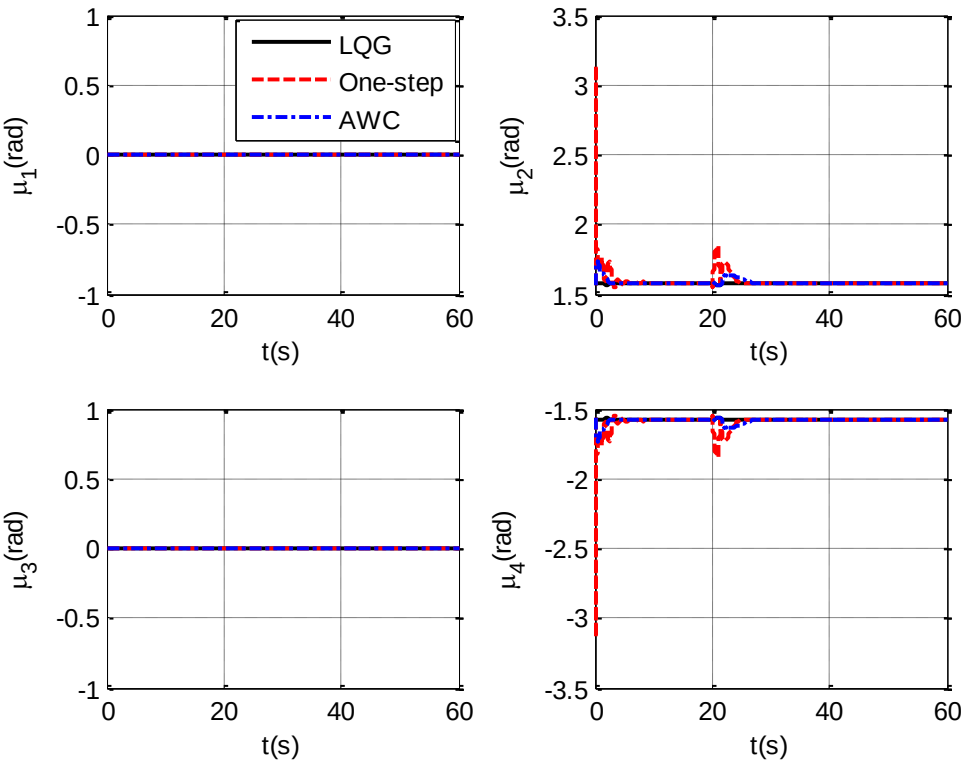

Fig.14 Time evolution of vectored angle (Second case without saturation)

In the second case, with even with smaller disturbances, saturation always occurred, because of the multi-channel coupling and the critical limits of the thrusts, which should be greater than zero as shown in Fig.13. However, we still can see that the AWC method almost acted as the nominal linear controller when saturation is not encountered, and the one-step approach still calculates an optimal solution within the constraints of a safe domain of operation. So the state responses of the one-step approach were smoother, however the output forces are relatively large compared with that of the other two methods as shown in Fig.12 and Fig.13.

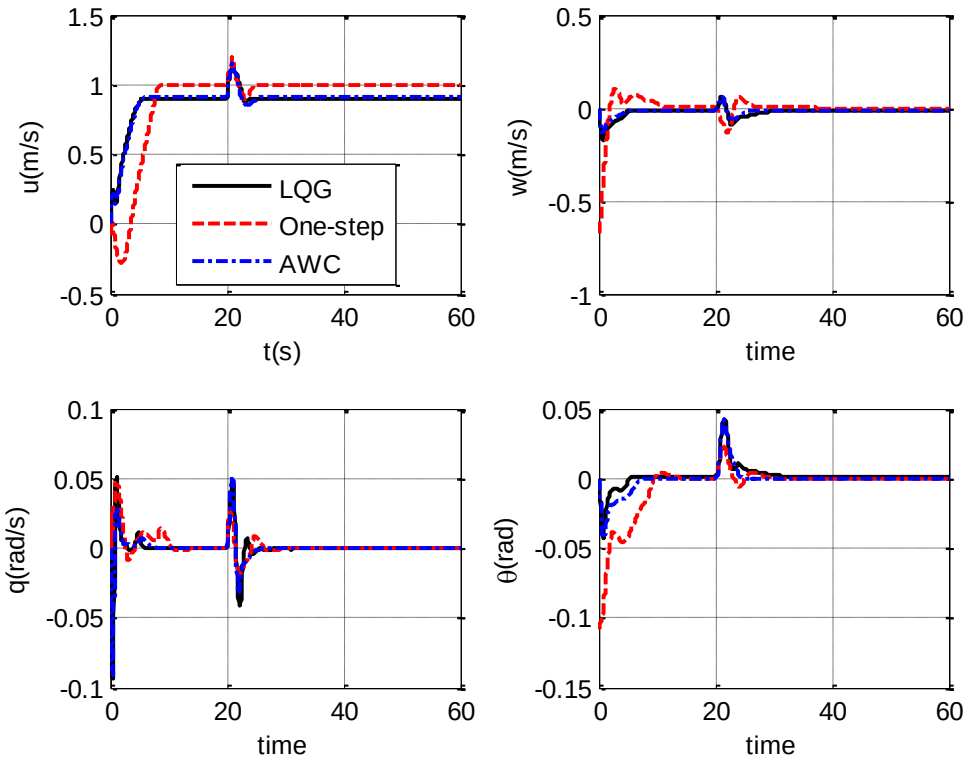

Fig.15 Time evolution of state (Third case based on nonlinear model)

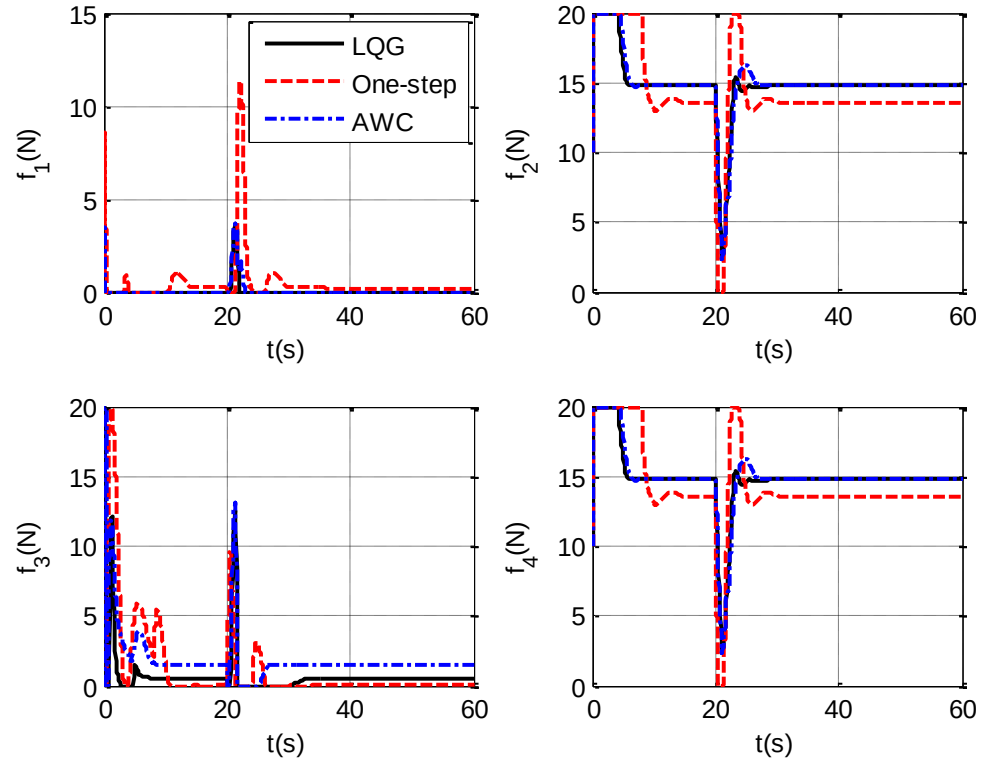

Fig.16 Time evolution of force (Third case third case based on nonlinear model)

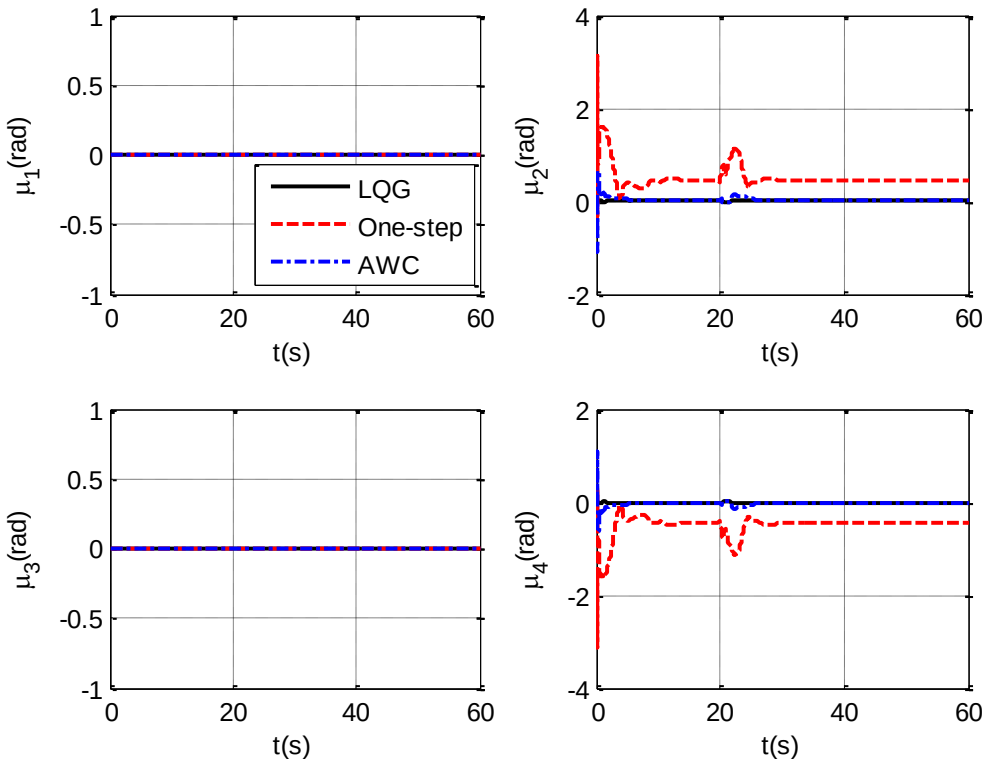

Fig.17 Time evolution of vectored angle (Third case third case based on nonlinear model)

In the final case, the nonlinear model is used for validation of the controller. Comparing the state responses of Fig.15 with that of Fig.10 and the input forces of Fig.16 with that of Fig.11, we can see the state response and the control input of the AWC is not very different to that of the LQG controller in the third case, but there is steady state error in u. The response of the vertical velocity w under the LQG controller based on the nonlinear model is better than that based on linear model, which is because the more accurate model gives some dynamic compensation. There is no steady error in the time response of one-step method based on different model, however the state response of the one-step method are a little worse in the initial phase. The actuator saturation of the one-step controller extends for longer time based on the nonlinear model than that based on the linear model.

5. Conclusion

Two methods for the control of the multi-vectored propeller airship are proposed. Both methods offer improvements on the LQG controller when the actuators are subject to saturation constraints. The strategies significantly increase the set of admissible initial states and drastically reduce the settling time. However although one-step controllers are satisfactory in principle, they have been criticized for their conservatism and lack of applicability to some practical problems because of the very high control gain matrix. The traditional anti-windup compensator is devoted to achieve nominal performance and constraint handling. It has smaller control matrix gains and small control saturation excesses, hence is more attractive in practice.

The research of this paper also highlights some limitations of the proposed methods: 1) For the LMI based saturated control problem, the stability is guaranteed by the inequality (23) and the performance is guaranteed by the minimization of the objective function (22) for given δ and τ_1. Through δ and τ_1 are adjustable, they make the methods conservative, because there are not always solutions for any combination of δ and τ_1. 2) In this paper the objective function has no direct relation with the tracking performance, so not all the possible solutions may guarantee the command tracking ability of command. 3) For MIMO systems, because of the coupled states, the region of stability and allowed states of saturation are hard to describe in an intuitive visual description. 4) The one-step method has the advantage of direct controller design for a saturated system, however the obtained region of stability in this example is very small, a more elaborate analysis can improve it further based on accurately modelling of the real system.

Acknowledgements

This work was supported by National Science Foundation of China, nos. 61175074 and 11272205.

References

1. Fossard AI and Normand-Cyrot D. *Nonlinear systems: stability and stabilization*. London: Chapman & Hall, 1996.

2. Tarbouriech S, Garcia G and Glattfelder AH. *Advanced strategies in control systems with input and output constraints*. LNCIS, vol.346, Springer Verlag, 2007.

3. Shtessel Y, Buffington J, Pachter M, et al. Reconfigurable flight control on sliding modes addressing actuator deflection and deflection rate. In: *AIAA Guidance, Navigation, and Control Conference and Exhibit*, Boston, MA, 10-12 August 1998; paper no. AIAA-98-4112, pp. 127-137.

4. Queinnec I, Tarbouriech S and Garcia G. Anti-windup design for aircraft control. In: *Proc. IEEE Conf. Control Applications (CCA)*, Munich, Germany, 2006:2541-2546.

5. Hu T and Lin ZL. Controlled invariance of ellipsoids: linear vs. nonlinear feedback. *Syst. Control Lett* 2004; 53(3-4): 203-210.

6. Benzaouia A. *Saturated Switched Systems*. LNCIS, vol.426, Springer Verlag. 2012.

7.Suárez R, Alvarez-Ramirez J and Solis-Daun J. Linear systems with bounded inputs: global stabilization with eigenvalue placement. *Int. J. Robust Nonlinear Control* 1997; 7(9): 835-845

8. Bemporad A, Teel AR and Zaccarian L. L_2 anti-windup via receding horizon optimal control. In: *2002 American Control Conference*, Anchorage, AK, 8-10 May 2002; pp. 639-644.

9. Hindi H and Boyd S. Analysis of linear systems with saturation using convex optimization. In: *Conference on Decision and Control* 1998; Tampa or, USA, pp. 903-908.

10. Wada N and Saeki M. An LMI based scheduling algorithm for constrained stabilization problems. *Syst. Control Lett* 2008; 57:255-261.

11. Palmeira AHK, Gomes da Silva JM, Tarbouriech S, et al. Sampled-data control under magnitude and rate saturating actuators. *Int. J. Robust Nonlinear Control* 2016; 26:3232-3252

12. Jungers M and Tarbouriech S. Anti-windup strategies for discrete-time switched systems subject to input saturation. *Int. J.* Control 2016; 89 (5): 1-29.

13.Tarbouriech S, Garcia G, Gomes da Silva JM, et al. *Stability and Stabilization of Linear Systems with Saturating Actuators*. London: Springer-Verlag, 2011.

14. Garcia G, Tarbouriech S, Gomes da Silva JM and Eckhard D. Finite L_2 gain and internal stabilization of linear systems subject to actuator and sensor saturations. *IET Control Theory and Appl.* 2009; 3(7): 799-812.

15. Gomes da Silva JM and Tarbouriech S. Local stabilization of discrete-time linear systems with saturating controls: an LMI-based approach. *IEEE Trans. Autom. Control* 2001; 46(1): 119-125.

16. Kapila V and Grigoriadis KM. *Actuator saturation control*. Marcel Dekker, New York, ISBN 0-8247-0751-6, 2002.

17. Hu TS and Lin ZL. *Control systems with actuator saturation: analysis and design*. Birkh¨auser, Boston, ISBN: 0-8176-4219-6, 2001.

18.Oliveira MZ, Gomes da Silva Jr JM, Coutinho D, et al. Anti-windup Design for a Class of Multivariable Nonlinear Control Systems: an LMI-based Approach. In: *50th IEEE Conference on Decision and Control and European Control Conference* (CDC-ECC), Orlando, FL, USA, December 12-15, 2011.

19. Grimm G, Hatfield J, Postlethwaite I, et al. Antiwindup for stable linear systems with input saturation: an LMI-based synthesis. *IEEE Trans. Autom. Control* 2003; 48(9): 1509-1525.

20. Tarbouriech S and Turner M. Anti-windup design: an overview of some recent advances and open problems. *IET Control Theory Appl.*, 2009; 3(1):1-19.

21. Sussmann HJ, Sontag ED and Yang Y. A general result on the stabilization of linear systems using bounded controls. *IEEE Trans. Autom. Control* 1994; 39(12): 2411-2425.

22. Gomes da Silva JM and Tarbouriech S. Anti-windup design with guaranteed regions of stability: an LMI-based Approach. *IEEE Trans. Autom. Control* 2005; 50(1): 106-111.

23. Boyd S, El Ghaoui L, Féron E and Balakrishnan V. *Linear Matrix Inequalities in System and Control Theory.* Philadelphia: SIAM, 1994.

24. Benzaouia A, Benhayoun M and Mesquine F. Stabilization of systems with unsymmetrical saturated control: an LMI approach. *Circuits Syst Signal Process* 2014; 33(10): 3263-3275.

25. Chen L, Zhang H and Duan DP. Control system design of a multi-vectored thrust stratospheric airship. *Proc IMechE Part G: J Aerospace Engineering* 2014; 228(11) 2045-2054.

2017-04-03

Application of Lyapunov matrix inequality based unsymmetrical saturated control to a multi-vectored propeller airship

Chen, Li

SAGE

Li Chen, James F Whidborne, Qi Dong, Deng Ping Duan. Application of Lyapunov matrix inequality based unsymmetrical saturated control to a multi-vectored propeller airship. Proceedings of the Institution of Mechanical Engineers, Part G: Journal of Aerospace þÿ E n g i n e e r i n g , 2 0 1 8 , V o l 2 3 2 , I s s u e 5 , p p 8 8 4 9 0 1
http://dx.doi.org/10.1177/0954410017699236